Modelling livestock

Julien Arino

April 2023

2023-04-17

Modelling livestock

Modelling livestock

Julien Arino

April 2023

Why?

Yes, why, really, must I tell you about this ?

I model the spread of infectious diseases and, less frequently, more general interactions between species (mathematical ecology)

I have even modelled how filaments grow (assemble) in cells

But “modelling livestock” ? Nope, never

So let’s take a (for the most part uninformed) dive in models of livestock

Why?

Yes, why, really, must I tell you about this ?

I model the spread of infectious diseases and, less frequently, more general interactions between species (mathematical ecology)

I have even modelled how filaments grow (assemble) in cells

But “modelling livestock” ? Nope, never

So let’s take a (for the most part uninformed) dive in models of livestock

Wait..

Digging through the literature, there's actually quite a lot and some of it is quite fun!

This will be a completely non-exhaustive and random review of some models I have found **excluding** anything infectious disease related

Wait..

Digging through the literature, there's actually quite a lot and some of it is quite fun!

This will be a completely non-exhaustive and random review of some models I have found **excluding** anything infectious disease related

Outline

Outline

Models for cattle

Models for other herds

Models for management

Conclusion

Models for cattle
Models for individuals
Models for herds
Models for other herds
Models for management
Conclusion

Models for cattle
Models for individuals
Models for herds
Models for other herds
Models for management
Conclusion

At the individual level

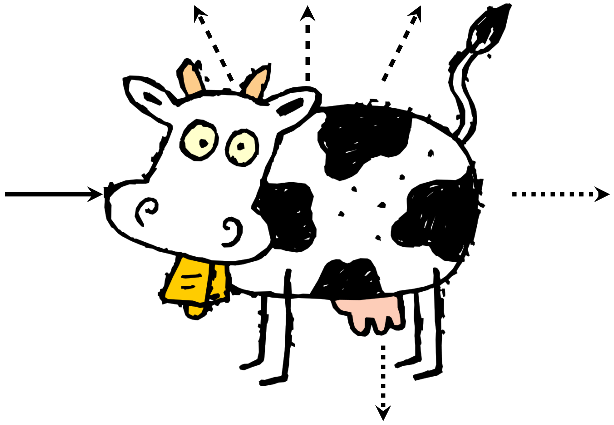

2023-04-17

Modelling livestock
└─Models for cattle
  └─Models for individuals
    └─At the individual level

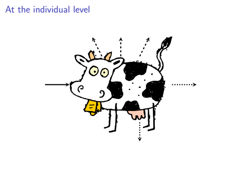

Journal of Agricultural Science (2010), **148**, 31–54. © *Cambridge University Press* 2009 31
doi:10.1017/S0021859609990244 *Printed in the United Kingdom*

MODELLING ANIMAL SYSTEMS PAPER

Development of a dynamic mathematical model for investigating mammary gland metabolism in lactating cows

V. VOLPE[1]*, J. P. CANT[2], R. C. BOSTON[3], P. SUSMEL[1] AND P. MOATE[3]†

[1] *Department of Animal Science, University of Udine, 33010 Pagnacco (Ud), Italy*
[2] *Centre for Nutrition Modelling, Department of Animal and Poultry Science, University of Guelph, Guelph, Ontario N1G2W1, Canada*
[3] *Biostatistics Section, Department of Clinical Studies, University of Pennsylvania, Kennet Square, PA 19348, USA*

(*Revised MS received 16 February 2009; First published online 3 September 2009*)

Journal of Agricultural Science (2010), 148, 31–54. © Cambridge University Press 2009 31
doi:10.1017/S0021859609990244 Printed in the United Kingdom
MODELLING ANIMAL SYSTEMS PAPER
Development of a dynamic mathematical model for investigating mammary gland metabolism in lactating cows
V. VOLPE[1]*, J. P. CANT[2], R. C. BOSTON[3], P. SUSMEL[1] AND P. MOATE[3]†
[1] Department of Animal Science, University of Udine, 33010 Pagnacco (Ud), Italy
[2] Centre for Nutrition Modelling, Department of Animal and Poultry Science, University of Guelph, Guelph, Ontario N1G2W1, Canada
[3] Biostatistics Section, Department of Clinical Studies, University of Pennsylvania, Kennet Square, PA 19348, USA
(Revised MS received 16 February 2009; First published online 3 September 2009)

Abbreviation	Meaning
Aa	Amino acids
AaE	Essential amino acids
AaN	Non-essential amino acids
Ac	Acetate
Acm	Mitochondrial acetyl-CoA
Adp	Adenosine-diphoshate
AP	Mammary tissue actively perfused
Atp	Adenosine-triphosphate
Bhb	β-hydroxybutyrate
Cit	Citrate
eAa	Amino acids in the arterial plasma
eAc	Acetate in the arterial plasma
eBhb	β-hydroxybutyrate in the arterial plasma
eGlc	Glucose in the arterial plasma
eFa	FAs in the arterial plasma
Fa	FAs
F6p	Fructose-6-phosphate
Fbp	Fructose-1,6-biphosphate
Glc	Glucose
G6p	Glucose-6-phosphate
Gcl	Glycerol
Lac	Lactose
Oa	Oxaloacetate
Pga	Phospho-glyceraldehyde
Ptm	Milk protein synthesized in the gland
Pyr	Pyruvate
R5p	Ribulose-5-phosphate
Succ	Succinate
Tca	Tricarboxylic acids
Tgm	Triacylglycerol in milk

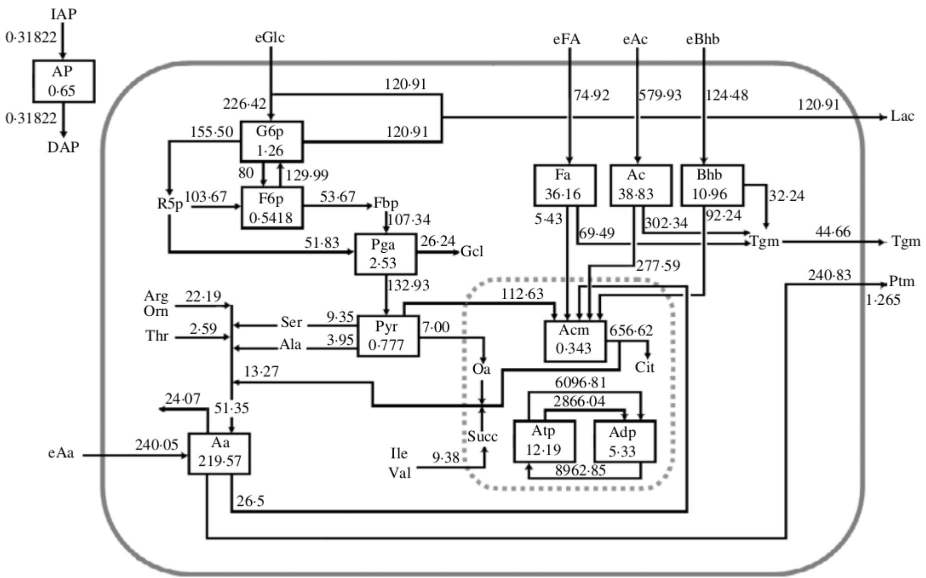

Fig. 1. Reference steady state diagram. Each individual compartment is represented through a box. Symbols are described in Table 2. AP is the volume of tissue actively perfused by blood. Fluxes are mmol/h except for IAP and DAP. Numbers in the boxes indicate the initial condition size of the compartment (mmol).

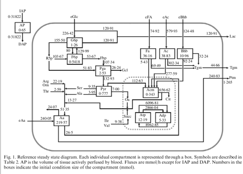

Notation	Meaning	Units
cA	Intracellular concentration of A	mmol/l
ceA	Arterial concentration of A	mmol/l
$^{\circ}$ceA	Reference arterial concentration of A	mmol/l
INSH	Insulinaemia	Units
J_{A}	Inhibition constant for the inflow of A	mmol/l
$J_{\mathrm{C,AB}}$	Inhibition constant for transaction A→B with respect to C	mmol/l
K_{InA}	Affinity constant for the inflow of A	mmol/l
K_{OutA}	Affinity constant for the outflow of A	mmol/l
$K_{\mathrm{A,B}}$	Affinity constant for A in the transaction A→B	mmol/l
$K_{\mathrm{C,AB}}$	Affinity constant for transaction A→B with respect to C	mmol/l
$P_{\mathrm{B,A}}$	Rate of synthesis of B in the transaction A→B	mmol/h
PPS	Potential milk protein yield	mmol/h
$R_{\mathrm{A,B}}$	Requirement of A in the synthesis of B	mmol/mmol
R_i	Content of *i*th AA in milk protein synthesized in the gland	mmol/mmol
RPS	Real milk protein yield	mmol/h
$U_{\mathrm{A,B}}$	Rate of utilization of A in the transaction A→B	mmol/h
$^{\circ}U_{\mathrm{A,B}}$	Reference rate of utilization of A in the transaction A→B	mmol/h
UO_i	Uptake:output ratio for the *i*th AA	mmol/mmol
UW	Udder weight	kg
$v_{\mathrm{eA,A}}$	Net uptake rate of A	mmol/h
$V_{\mathrm{A,B}}$	$V_{\max}$ for the transaction A→B	mmol/h
V_{InA}	$V_{\max}$ for the inflow of A	µmol/l
V_{OutA}	$V_{\max}$ for the outflow of A	µmol/l
$Y_{\mathrm{A,B}}$	Rate of yield of B in the transaction A→B	mmol/mmol

Table 4. *MM parameters of the equations describing uptakes of nutrients*

Equation no.	V_{InA} (μmol/l)	K_{InA} (mM)	K_{InB} (mM)	J_{A} (mM)	V_{outA} (μmol/l)	K_{outA} (mM)
(2.2): Arg	135·610	0·095	–	12·158	22·600	12·158
(2.2): His	49·060	0·053	–	12·158	8·200	12·158
(2.2): Ile	164·920	0·101	–	12·158	27·490	12·158
(2.2): Leu	232·0	0·065	–	12·158	62·500	12·158
(2.2): Lys	282·120	0·125	–	12·158	47·020	12·158
(2.2): Met	50·990	0·025	–	12·158	8·500	12·158
(2.2): Phe	85·490	0·039	–	12·158	14·250	12·158
(2.2): Thr	127·710	0·080	–	12·158	21·290	12·158
(2.2): Trp	18·990	0·047	–	12·158	3·170	12·158
(2.2): Val	215·330	0·147	–	12·158	35·890	12·158
(2.9): Ala	67·370	0·189	–	12·158	11·230	12·158
(2.9): Asp	10·540	0·004	–	12·158	1·0	12·158
(2.9): Asn	127·230	0·129	–	12·158	21·210	12·158
(2.9): Cys	36·340	0·045	–	12·158	6·060	12·158
(2.9): Glu	159·480	0·058	–	12·158	15·190	12·158
(2.9): Gln	134·270	0·221	–	12·158	22·380	12·158
(2.9): Gly	30·550	0·231	–	12·158	5·090	12·158
(2.9): Pro	34·020	0·110	–	12·158	5·671	12·158
(2.9): Ser	95·230	0·084	–	12·158	15·870	12·158
(2.9): Tyr	77·300	0·045	–	12·158	12·880	12·158
(2.9): Orn	133·690	0·073	–	12·158	22·280	12·158
(3.1): Ac*	3·600	2·150	–	–	0·450	0·253
(5.1): Bhb*	1·250	0·750	–	–	0·550	0·420
(6.1): Fa*†	1·100	0·280	0·100	–	0·150	0·309
(7.1): Glc*‡	2·250	3·640	–	–	1·250	0·081

* For Ac, Bhb, Fa and Glc parameters V_{InA} and V_{outA} are expressed in mmol/l.
† Equation (6.1), K_{InA} and K_{InB} are K_{InNefa} and K_{InTg} respectively.
‡ Equation (7.1), parameters V_{InA}, K_{InA}, V_{outA} and K_{outA} are $V_{\mathrm{eGlc,G6p}}$, $K_{\mathrm{eGlc,G6p}}$, $V_{\mathrm{G6p,eGlc}}$ and $K_{\mathrm{G6p,eGlc}}$, respectively.

APPENDIX

MATHEMATICAL STATEMENT OF THE MODEL

Mammary plasma flow

$$\mathrm{dAP}/\mathrm{d}t = \mathrm{IAP} - \mathrm{DAP} \tag{1.0}$$

– *Inputs*:

$$\mathrm{IAP} = \mathrm{PPS}/\mathrm{MIN}\{\mathrm{RPS},\ \mathrm{PPS}\}\ \mathrm{INSH}^{\mathbf{0{\cdot}20}} 0{\cdot}350/(1 + 0{\cdot}035/(1 - \mathrm{AP})) \tag{1.1}$$

– *Outputs*:

$$\mathrm{DAP} = \mathrm{cAtp}/\mathrm{cAdp}\ 0{\cdot}1522/(1 + 0{\cdot}065/\mathrm{AP}) \tag{1.2}$$

$$\mathrm{MPF} = \mathrm{MS}^{\circ} 0{\cdot}9974^{(\mathrm{DIM} - \mathbf{133})}\mathrm{UW753AP} \tag{1.3}$$

AA compartment (*Aa*)

$$\mathrm{dAa}/\mathrm{d}t = v_{\mathrm{eAa,\,Aa}} + P_{\mathrm{AaN,\,AaE}} - U_{\mathrm{Aa,\,Deg}} - U_{\mathrm{Aa,\,Mtb}} - U_{\mathrm{Aa,\,Ptm}} \tag{2.0}$$

– *Inputs*:

$$v_{\mathrm{eAa,\,Aa}} = \sum v_{\mathrm{eAaEi,\,AaEi}} + \sum v_{\mathrm{eAaNi,\,AaNi}} \tag{2.1}$$

Uptake of essential AAs

$$\begin{aligned} v_{\mathrm{eAaEi,\,AaEi}} = {} & V_{\mathrm{InAai}}\mathrm{MPF}({}^{\circ}\mathrm{ceAaE}_i/\mathrm{ceAaE}_i)^{\mathbf{0{\cdot}2}}/(1 + K_{\mathrm{InAai}}(\mathrm{oRPS}_i/\mathrm{ePS})^{\varepsilon}/\mathrm{ceAaE}_i + (\mathrm{cAa}/J_{\mathrm{Aa}})^{\mathbf{3{\cdot}5}}) \\ & - V_{\mathrm{OutAai}}\mathrm{MPF}/(1 + K_{\mathrm{OutAa}}/\mathrm{cAa}) \end{aligned} \tag{2.2}$$

$$\begin{aligned} \mathrm{oRPS}_{\mathrm{His}} = {} & \{V_{\mathrm{InHis}}\mathrm{MPF}({}^{\circ}\mathrm{ceHis}/\mathrm{ceHis})^{\mathbf{0{\cdot}2}}/(1 + K_{\mathrm{InHis}}/\mathrm{ceHis} + (\mathrm{cAa}/J_{\mathrm{Aa}})^{\mathbf{3{\cdot}5}}) \\ & - V_{\mathrm{OutHis}}\mathrm{MPF}/(1 + K_{\mathrm{OutAa}}/\mathrm{cAa})\}\mathbf{1{\cdot}1}/(\mathrm{UO}_{\mathrm{His}}R_{\mathrm{His}}) \end{aligned} \tag{2.3}$$

$$\begin{aligned}\mathrm{oRPS_{Met}} = \{&V_{\mathrm{InMet}}\mathrm{MPF}(^{\circ}\mathrm{ceMet}/\mathrm{ceMet})^{\mathbf{0\cdot 2}}/(1+K_{\mathrm{InMet}}/\mathrm{ceMet}+(\mathrm{cAa}/J_{\mathrm{Aa}})^{\mathbf{3\cdot 5}}) \\ &- V_{\mathrm{OutMet}}\mathrm{MPF}/(1+K_{\mathrm{OutAa}}/\mathrm{cAa})\}1\cdot 1/(\mathrm{UO_{Met}}R_{\mathrm{Met}})\end{aligned} \tag{2.4}$$

$$\begin{aligned}\mathrm{oRPS_{Phe}} = \{&V_{\mathrm{InPhe}}\mathrm{MPF}(^{\circ}\mathrm{cePhe}/\mathrm{cePhe})^{\mathbf{0\cdot 2}}/(1+K_{\mathrm{InPhe}}/\mathrm{cePhe}+(\mathrm{cAa}/J_{\mathrm{Aa}})^{\mathbf{3\cdot 5}}) \\ &- V_{\mathrm{OutPhe}}\mathrm{MPF}/(1+K_{\mathrm{OutAa}}/\mathrm{cAa})\}1\cdot 1/(\mathrm{UO_{Phe}}R_{\mathrm{Phe}})\end{aligned} \tag{2.5}$$

$$\begin{aligned}\mathrm{oRPS_{Leu}} = \{&V_{\mathrm{InLeu}}\mathrm{MPF}(^{\circ}\mathrm{ceLeu}/\mathrm{ceLeu})^{\mathbf{0\cdot 2}}/(1+K_{\mathrm{InLeu}}/\mathrm{ceLeu}+(\mathrm{cAa}/J_{\mathrm{Aa}})^{3\cdot 5}) \\ &- V_{\mathrm{OutLeu}}\mathrm{MPF}/(1+K_{\mathrm{OutAa}}/\mathrm{cAa})\}/(\mathrm{UO_{Leu}}R_{\mathrm{Leu}})\end{aligned} \tag{2.6}$$

$$\mathrm{oRPS_{AaO}} = \mathrm{MIN}\{\mathrm{oRPS_{His}}, \mathrm{oRPS_{Met}}, \mathrm{oRPS_{Phe}}\} \tag{2.7}$$

$$\mathrm{ePS} = \mathrm{PPS\ INSH}^{\mathbf{0\cdot 050}} \tag{2.8}$$

Uptake of non-essential AAs

$$\begin{aligned}v_{\mathrm{eAaNi,\,AaNi}} = &V_{\mathrm{InAai}}\mathrm{MPF}(^{\circ}\mathrm{ceAaN}_i/\mathrm{ceAaN}_i)^{\mathbf{0\cdot 2}}/(1+K_{\mathrm{InAai}}/\mathrm{ceAaN}_i+(\mathrm{cAa}/J_{\mathrm{Aa}})^{\mathbf{3\cdot 5}}) \\ &- V_{\mathrm{OutAai}}\mathrm{MPF}/(1+K_{\mathrm{OutAai}}/\mathrm{cAa})\end{aligned} \tag{2.9}$$

Synthesis of non-essential AAs

$$P_{\mathrm{AaN,\,AaE}} = U_{\mathrm{Pyr,\,Ser}} + U_{\mathrm{Pyr,\,Ala}} + P_{\mathrm{GlAs,\,AaE}} + P_{\mathrm{Pro,\,Arg}} + P_{\mathrm{Gly,\,Thr}} \tag{2.10}$$

$$U_{\mathrm{Pyr,\,Ser}} = (\mathrm{RPS}\ R_{\mathrm{Ser}} - v_{\mathrm{eSer,\,Ser}} + \mathrm{RPS}\ R_{\mathrm{Gly}} - v_{\mathrm{eGly,\,Gly}}) * V_{\mathrm{Pyr,\,Ser}}/(1+K_{\mathrm{Pyr,\,Ser}}/\mathrm{cPyr}) \tag{2.11}$$

$$U_{\mathrm{Pyr,\,Ala}} = (\mathrm{RPS}\ R_{\mathrm{Ala}} - v_{\mathrm{eAla,\,Ala}})V_{\mathrm{Pyr,\,Ala}}/(1+K_{\mathrm{Pyr,\,Ala}}/\mathrm{cPyr}) \tag{2.12}$$

$$P_{\mathrm{GlAs,\,AaE}} = 0\cdot 019717(U_{\mathrm{Pyr,\,Oa}} + U_{\mathrm{Acm,\,Cit}} + U_{\mathrm{Val,\,SuccTca}} + U_{\mathrm{Ile,\,SuccTca}}) \tag{2.13}$$

$$U_{\mathrm{Val,\,SuccTca}} = v_{\mathrm{eVal,\,Val}} - \mathrm{RPS}\ R_{\mathrm{Val}} \tag{2.14}$$

$$U_{\mathrm{Ile,\,SuccTca}} = v_{\mathrm{eIle,\,Ile}} - \mathrm{RPS}\ R_{\mathrm{Ile}} \tag{2.15}$$

$$P_{\mathrm{Pro,\,Arg}} = \mathrm{RPS}\ R_{\mathrm{Pro}} - v_{\mathrm{ePro,\,Pro}} \tag{2.16}$$

$$P_{\mathrm{Gly,\,Thr}} = \mathrm{RPS}\ R_{\mathrm{Gly}} - v_{\mathrm{eGly,\,Gly}} + \mathrm{RPS}\ R_{\mathrm{Ser}} - U_{\mathrm{Pyr,\,Ser}} - v_{\mathrm{eSer,\,Ser}} \tag{2.17}$$

– *Outputs*:

$$U_{\mathrm{Aa,\,Deg}} = V_{\mathrm{Aa,\,Deg}}/((1+(\mathrm{INSH}/5)^{0\cdot30})(1+(K_{\mathrm{Aa,\,Deg}}/\mathrm{cAa})^{2\cdot50})) \tag{2.18}$$

$$U_{\mathrm{Aa,\,Mtb}} = (v_{\mathrm{eArg,\,Arg}} - \mathrm{RPS}\ R_{\mathrm{Arg}} + v_{\mathrm{eOrn,\,Orn}})V_{\mathrm{Aa,\,Mtb}}/(1+(K_{\mathrm{Aa,\,Mtb}}/\mathrm{cAa})^{2\cdot50}) \tag{2.19}$$

$$U_{\mathrm{Aa,\,Ptm}} = \mathrm{RPS}\ V_{\mathrm{Aa,\,Ptm}}/(1+K_{\mathrm{Aa,\,Ptm}}/\mathrm{cAa}) \tag{2.20}$$

$$\mathrm{RPS} = P_{\mathrm{Ptm,\,Aa}}\ \ Y_{\mathrm{Atp,\,Ptm}} \tag{2.21}$$

$$P_{\mathrm{Ptm,\,Aa}} = \mathrm{MIN}\{1\cdot09 v_{\mathrm{eHis,\,His}}/R_{\mathrm{His}};\ 1\cdot09 v_{\mathrm{eMet,\,Met}}/R_{\mathrm{Met}};\ 1\cdot09 v_{\mathrm{ePhe,\,Phe}}/R_{\mathrm{Phe}}\} \tag{2.22}$$

$$Y_{\mathrm{Atp,\,Ptm}} = \mathrm{MIN}\{1\cdot000;\ V_{\mathrm{Atp,\,Ptm}}/(1+K_{\mathrm{Atp,\,Ptm}}/\mathrm{cAtp})\} \tag{2.23}$$

Acetate compartment (Ac)

$$\mathrm{dAc}/\mathrm{d}t = v_{\mathrm{eAc,\,Ac}} - U_{\mathrm{Ac,\,Acm}} - U_{\mathrm{Ac,\,Tgm}} \tag{3.0}$$

– *Inputs*:

$$v_{\mathrm{eAc,\,Ac}} = V_{\mathrm{InAc}}\mathrm{MPF}/(1+K_{\mathrm{InAc}}/\mathrm{ceAc}) - V_{\mathrm{OutAc}}\mathrm{MPF}/(1+K_{\mathrm{OutAc}}/\mathrm{cAc}) \tag{3.1}$$

Animal Nutrition 1 (2015) 329–338

Contents lists available at ScienceDirect

Animal Nutrition

journal homepage: http://www.keaipublishing.com/en/journals/aninu/

Original research article

A mathematical model to describe the diurnal pattern of enteric methane emissions from non-lactating dairy cows post-feeding

Min Wang [a], Rong Wang [a], Xuezhao Sun [b], Liang Chen [a], Shaoxun Tang [a], Chuangshe Zhou [a], Xuefeng Han [a], Jinghe Kang [a], Zhiliang Tan [a,*], Zhixiong He [a]

[a] Key Laboratory for Agro-Ecological Processes in Subtropical Region, Hunan Research Center of Livestock & Poultry Sciences, South-Central Experimental Station of Animal Nutrition and Feed Science in the Ministry of Agriculture, Institute of Subtropical Agriculture, The Chinese Academy of Sciences, Changsha 410125, China

[b] Grasslands Research Centre, AgResearch Limited, Palmerston North 4442, New Zealand

Original research article

A mathematical model to describe the diurnal pattern of enteric methane emissions from non-lactating dairy cows post-feeding

2.1. The model

The parameters for the model development are summarized in Table 1. Methane is emitted during the metabolism of methanogens that use hydrogen as an energy source, and this hydrogen is produced mainly during fermentation of degradable substrate by microorganisms in the rumen (Wang et al., 2013a). Methane emission rate (dV/dt, g/h) is assumed to be proportional to methanogen mass (M_r, g), activity of methanogens and degradable substrate (S_r, g) in the rumen, and is expressed as:

$$\frac{dV}{dt} = \alpha\beta_M M_r S_r, \tag{1}$$

where α is a proportionality constant [/(h·g)], β_M is the activity of methanogens linking the methane production and methanogen mass (g/g).

The substrate in the rumen was separated into two components: newly ingested and the residue, representing potential nutrient sources from the current and previous feeding, respectively. The total enteric methane produced associated with these feed fractions was a combination of that produced from use of residual (basal) substrate (V_1) and newly ingested (V_2) feed in the rumen.

2.1. The model

The parameters for the model development are summarized in Table 1. Methane is emitted during the metabolism of methanogens that use hydrogen as an energy source, and this hydrogen is produced mainly during fermentation of degradable substrate by microorganisms in the rumen (Wang et al., 2013a). Methane emission rate (dV/dt, g/h) is assumed to be proportional to methanogen mass (M_r, g), activity of methanogens and degradable substrate (S_r, g) in the rumen, and is expressed as:

$$\frac{dV}{dt} = \alpha\beta_M M_r S_r. \tag{1}$$

where α is a proportionality constant [/(h·g)], β_M is the activity of methanogens linking the methane production and methanogen mass (g/g).

The substrate in the rumen was separated into two components: newly ingested and the residue, representing potential nutrient sources from the current and previous feeding, respectively. The total enteric methane produced associated with these feed fractions was a combination of that produced from use of residual (basal) substrate (V_1) and newly ingested (V_2) feed in the rumen.

that changes in methane emissions are a response to substrate supply and activity of the methanogens, while methanogen mass (M_r) was assumed fixed for an individual animal on a particular ration. The rate of enteric methane emission, thus, can be expressed as follows:

$$\frac{\mathrm{d}V}{\mathrm{d}t} = \frac{\mathrm{d}V_1}{\mathrm{d}t} + \frac{\mathrm{d}V_2}{\mathrm{d}t}, \tag{2}$$

$$\frac{\mathrm{d}V_1}{\mathrm{d}t} = \alpha_1 \beta_{M1} M_r S_{rr}, \tag{2a}$$

$$\frac{\mathrm{d}V_2}{\mathrm{d}t} = \alpha_2 \beta_{M2} M_r S_{Ir}, \tag{2b}$$

where α_1 and α_2 are proportionality constants [/(h·g)] for basal V_1 and feeding V_2, respectively; β_{M1} is the activity of methanogens to generate basal V_1; S_{rr} is the amount of degradable substrate in the residue of rumen before feeding (g); β_{M2} is the activity of methanogens to generate feeding V_2; S_{Ir} is the amount of degradable substrate in the rumen from the newly ingested feed (g).

that changes in methane emissions are a response to substrate supply and activity of the methanogens, while methanogen mass (M_r) was assumed fixed for an individual animal on a particular ration. The rate of enteric methane emission, thus, can be expressed as follows:

$$\frac{\mathrm{d}V}{\mathrm{d}t} = \frac{\mathrm{d}V_1}{\mathrm{d}t} + \frac{\mathrm{d}V_2}{\mathrm{d}t}, \tag{2}$$

$$\frac{\mathrm{d}V_1}{\mathrm{d}t} = \alpha_1 \beta_{M1} M_r S_{rr}, \tag{2a}$$

$$\frac{\mathrm{d}V_2}{\mathrm{d}t} = \alpha_2 \beta_{M2} M_r S_{Ir}, \tag{2b}$$

where α_1 and α_2 are proportionality constants [/(h·g)] for basal V_1 and feeding V_2, respectively; β_{M1} is the activity of methanogens to generate basal V_1; S_{rr} is the amount of degradable substrate in the residue of rumen before feeding (g); β_{M2} is the activity of methanogens to generate feeding V_2; S_{Ir} is the amount of degradable substrate in the rumen from the newly ingested feed (g).

Term	Unit	Explanation
V	g	Volume of enteric methane emission
V_1	g	Volume of enteric methane emission generated by the residual substrate in the rumen
V_2	g	Volume of enteric methane emission generated by the newly ingested feed
$\mathrm{d}V/\mathrm{d}t$	g/h	Rate of enteric methane emission
$\mathrm{d}V_1/\mathrm{d}t$	g/h	Rate of enteric methane emission for basal V_1
$\mathrm{d}V_2/\mathrm{d}t$	g/h	Rate of enteric methane emission for feeding V_2
α	/(h·g)	Proportionality constant
α_1	/(h·g)	Proportionality constant for basal V_1
α_2	/(h·g)	Proportionality constant for feeding V_2
β_M	—	Activity of methanogens
β_{M1}	—	Activity of methanogens to generate basal V_1
β_{M2}	—	Activity of methanogens to generate feeding V_2
S_r	g	Degradable Substrate in the rumen
S_{rr}	g	Degradable substrate in the residue in the rumen before feeding
S_{Ir}	g	Degradable substrate in the rumen from the newly ingested feed
S_I	g	Degradable substrate from newly ingested feed
S_{Ie}	g	Degradable substrate from newly ingested feed which outflow from rumen
M_r	g	Methanogens in the rumen
k_p	/h	Ruminal passage rates
S_T	g	Potential degradable substrate in the newly ingested feed
VF_2	g	Final asymptotic accumulated enteric methane emissions for feeding V_2
γ	g/h	Shape parameter
d	—	Shape parameter
a	g	Shape parameter

Summary of variables for non-lactating dairy cows ($n = 16$).

Item	Mean	Median	Minimum	Maximum	SD
BW, kg	222	215	98	420	110
DMI, kg/d	4.45	4.44	2.66	7.35	1.38
DMI_a :DMI_m ratio	0.957	0.987	0.854	1.040	0.085
Concentrate, kg/d	2.96	3.22	1.61	4.02	0.82
Rice straw, kg/d	1.48	1.26	0.83	3.39	0.703
Concentrate proportion in the diet, %	66.8	68.2	53.9	78.8	7.55
NDFI, kg/d	2.30	2.20	1.37	4.14	0.781
ADFI, kg/d	1.18	1.09	0.70	2.23	0.426
CPI, kg/d	0.553	0.571	0.319	0.827	0.159
GEI, MJ/d	72.3	72.3	43.2	119	22.3
Methane, g/d	88.3	82.2	42.6	170	38.0
Methane, % of GEI	6.59	6.44	5.11	8.04	1.00

BW = body weight; DMI = dry matter intake; DMI_m = DMI for morning feeding from 0600 to 1600 h; DMI_a = DMI for afternoon feeding from 1600 to 0600 h; NDFI = neutral detergent fibre intake; ADFI = acid detergent fiber intake; CPI = crude protein intake; GEI = gross energy intake; SD = standard deviation.

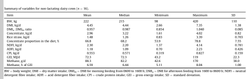

2.2. *Animal and housing*

The use of the animals and the experimental procedure were approved by the Animal Care Committee, Institute of Subtropical Agriculture. The experiment was conducted at a local farm in the Wang-Cheng County of Hunan Province, China. Sixteen non-lactating Chinese Holstein dairy cows with a wide range of BW (Table 2) were assigned to the air-flow controlled chamber for enteric methane emission measurement.

Cows were housed in a tie-stall dairy barn, and were accustomed to restricted movement. Both gaseous exchange and feed intake were individually determined when the cow was placed in the respiration chamber. Cows were allocated to the single respiration chamber for two consecutive days in a staggered manner. The data presented are averaged from the two days of chamber. The experiment lasted from early Feb. 2012 to late Apr. 2013.

2.2. Animal and housing

The use of the animals and the experimental procedure were approved by the Animal Care Committee, Institute of Subtropical Agriculture. The experiment was conducted at a local farm in the Wang-Cheng County of Hunan Province, China. Sixteen non-lactating Chinese Holstein dairy cows with a wide range of BW (Table 2) were assigned to the air-flow controlled chamber for enteric methane emission measurement.

Cows were housed in a tie-stall dairy barn, and were accustomed to restricted movement. Both gaseous exchange and feed intake were individually determined when the cow was placed in the respiration chamber. Cows were allocated to the single respiration chamber for two consecutive days in a staggered manner. The data presented are averaged from the two days of chamber. The experiment lasted from early Feb. 2012 to late Apr. 2013.

2.3. *Diet and feeding*

The diet consisted of concentrate and roughage (rice straw). The concentrate contained maize, soybean meal, cottonseed meal and corn distiller's dried grains and maize with solubles, purchased from Agribrands Purina Feed mill Co., Ltd. The chemical composition of the concentrate was 950 g DM/kg and 155 g of CP, 415 g of neutral detergent fibre (NDF) and 157 g of acid detergent fibre (ADF) per kg of DM. The chemical composition for the rice straw was (on a DM basis) 975 g/kg DM, 63 g/kg CP, 760 g/kg NDF and 466 g/kg ADF.

The allowances of concentrate and roughage were decided by the farmer, based on experience and according to the live weight of individual cows (each around 1% of live weight). As a result, the amount of concentrate supplied was different for each animal (Table 2). The concentrate and roughage were placed in two separate feeding troughs, with the concentrate provided first. All animals had ad libitum access to water. The restricted supply of concentrate was divided into two portions for the morning and afternoon feeds (0600 and 1605 h) while the rice straw was provided in slight excess for both periods. Orts were collected twice daily before the new feed was provided. The characteristics of feed intake for all animals are shown in Table 2.

2.3. Diet and feeding

The diet consisted of concentrate and roughage (rice straw). The concentrate contained maize, soybean meal, cottonseed meal and corn distiller's dried grains and maize with solubles, purchased from Agribrands Purina Feed mill Co., Ltd. The chemical composition of the concentrate was 950 g DM/kg and 155 g of CP, 415 g of neutral detergent fibre (NDF) and 157 g of acid detergent fibre (ADF) per kg of DM. The chemical composition for the rice straw was (on a DM basis) 975 g/kg DM, 63 g/kg CP, 760 g/kg NDF and 466 g/kg ADF.

The allowances of concentrate and roughage were decided by the farmer, based on experience and according to the live weight of individual cows (each around 1% of live weight). As a result, the amount of concentrate supplied was different for each animal (Table 2). The concentrate and roughage were placed in two separate feeding troughs, with the concentrate provided first. All animals had ad libitum access to water. The restricted supply of concentrate was divided into two portions for the morning and afternoon feeds (0600 and 1605 h) while the rice straw was provided in slight excess for both periods. Orts were collected twice daily before the new feed was provided. The characteristics of feed intake for all animals are shown in Table 2.

2.4. Measurement of methane emissions

One simple respiration chamber was built for the measurement of methane emissions from cows. Briefly, the chamber was made of galvanized steel plate with internal dimensions of 3 m length × 2 m width × 2 m height. The chamber had one front and one rear door

2.4. Measurement of methane emissions
One simple respiration chamber was built for the measurement of methane emissions from cows. Briefly, the chamber was made of galvanized steel plate with internal dimensions of 3 m length × 2 m width × 2 m height. The chamber had one front and one rear door

fitted with internal rubber seals. The cow was restrained in the chamber with access to a feed bin and a drinking water container. A fresh air inlet was located at the top left of the chamber, and air inlets were piped from an intake vent, located 15 m from the chamber. The outlet consisted of two round polyethylene pipes (outside diameter, 50 mm) fixed to the left and right insides of the chamber, and each pipe comprised of 50 intake holes equally distributed around the entire circumference of the duct. These two ducts were piped through the right side of chamber via a 50 mm outside diameter polyethylene pipe. The outlet was connected via a 50 mm air filter, to a gas flow meter, followed by the pump. Airflow (150 to 190 m^3/h) under negative pressure was controlled by the pump. The chamber was fitted with four internal ventilation fans for efficient mixing of exhaled gases and incoming air. The outlet pipe from the chamber was connected to a plastic buffer box (50 cm length $\times$ 50 cm width $\times$ 50 cm height) for gas sampling.

The outlet gas was sampled from the box every 15 min during 0600 to 2200 h, at 2300, 2400 h, next day 0200 and 0530 h. A 50-mL syringe was used for sampling, and then injected into a vacuum tube for methane determination by gas chromatography (Agilent 7890A, Agilent Inc., Palo Alto, CA).

The cows were placed in the chamber at 0600 h. The cows were fed after entering the chamber at 0600 h, and the chamber was opened once a day at 1605 h for 5 min to deliver diet. The first sample of outlet gas was collected after the cows had been shut in the chamber for 10 min. Three inlet gas samples were collect at 0600, 1200 and 1700 h, and their mean value used to represent the methane concentration of the inflowing air.

fitted with internal rubber seals. The cow was restrained in the chamber with access to a feed bin and a drinking water container. A fresh air inlet was located at the top left of the chamber, and air inlets were piped from an intake vent, located 15 m from the chamber. The outlet consisted of two round polyethylene pipes (outside diameter, 50 mm) fixed to the left and right insides of the chamber, and each pipe comprised of 50 intake holes equally distributed around the entire circumference of the duct. These two ducts were piped through the right side of chamber via a 50 mm outside diameter polyethylene pipe. The outlet was connected via a 50 mm air filter, to a gas flow meter, followed by the pump. Airflow (150 to 190 m^3/h) under negative pressure was controlled by the pump. The chamber was fitted with four internal ventilation fans for efficient mixing of exhaled gases and incoming air. The outlet pipe from the chamber was connected to a plastic buffer box (50 cm length $\times$ 50 cm width $\times$ 50 cm height) for gas sampling.

The outlet gas was sampled from the box every 15 min during 0600 to 2200 h, at 2300, 2400 h, next day 0200 and 0530 h. A 50-mL syringe was used for sampling, and then injected into a vacuum tube for methane determination by gas chromatography (Agilent 7890A, Agilent Inc., Palo Alto, CA).

The cows were placed in the chamber at 0600 h. The cows were fed after entering the chamber at 0600 h, and the chamber was opened once a day at 1605 h for 5 min to deliver diet. The first sample of outlet gas was collected after the cows had been shut in the chamber for 10 min. Three inlet gas samples were collect at 0600, 1200 and 1700 h, and their mean value used to represent the methane concentration of the inflowing air.

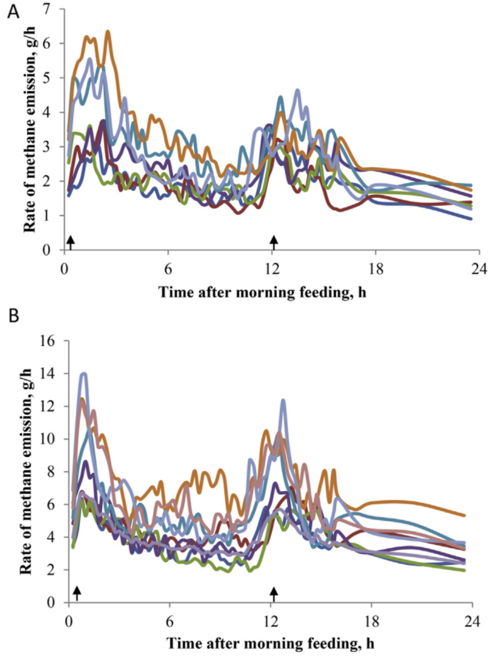

Fig. 1. Methane emission pattern (g/h) from sixteen non-lactating dairy cows for 24 h. Arrow was the time when the feed was provided. A and B were eight non-lactating dairy cows with body weight from 0 to 200 kg and 200 to 400 kg, respectively.

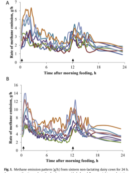

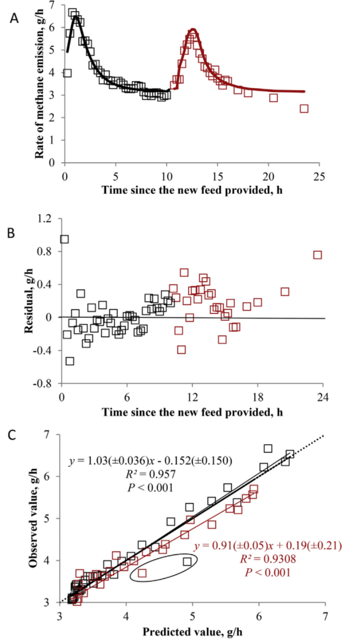

Fig. 2. Predicted versus observed rate of enteric methane emission. The observed and predicted rates of enteric methane emission are the average of 16 curves. A dotted line is unity of 1:1. Two points in the ellipse show disparity from the regression line. The data after morning and afternoon feeding were colored with black and red respectively. A and B were the diurnal pattern of rate of methane emissions and residual, respectively; C was predicted versus observed rate of enteric methane emission.

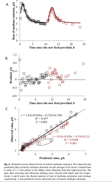

Animal Production Science, 2014, **54**, 1927–1938
http://dx.doi.org/10.1071/AN14533

Development of mathematical models to predict volume and nutrient composition of fresh manure from lactating Holstein cows

J. A. D. Ranga Niroshan Appuhamy[A,E], *L. E. Moraes*[A], *C. Wagner-Riddle*[B], *D. P. Casper*[C], *J. France*[D] *and E. Kebreab*[A]

[A]Department of Animal Science, University of California, Davis, CA 95616, USA.
[B]School of Environmental Sciences, University of Guelph, Guelph, ON, N1G 2W1, Canada.
[C]Department of Dairy Science, South Dakota State University, Brookings, SD 57007, USA.
[D]Centre for Nutrition Modelling, Department of Animal and Poultry Science, University of Guelph, Guelph, ON, N1G 2W1, Canada.
[E]Corresponding author. Email: jaappuhamy@ucdavis.edu

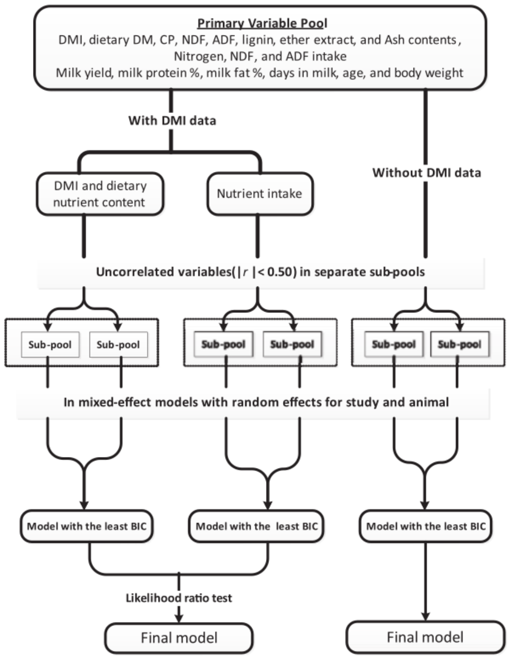

Fig. 1. Schematic diagram illustrating variable and model selection schemes.

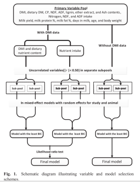

Table 5. Prediction equations (standard errors of parameters in parentheses), maximum variance inflation factor (max_VIF) and the determinant of the correlation matrix (*det*{R}) of the selected variables

F_{DM} = faecal dry matter, F_C = faecal carbon, F_{NDF} = faecal neutral detergent fibre (NDF), F_{ADF} = faecal acid detergent fibre (ADF), F_N = faecal nitrogen, F_{Water} = faecal water, U_E = total urine, U_C = urine carbon, and U_N = urine nitrogen outputs (all in kg/day). DMI = dry matter intake (kg/day), *CP*, *ADF*, *NDF* and *LIG* = dietary crude protein, ADF, NDF and lignin content, respectively (% of DM). Milk = milk yield (kg/day), mPrt = milk protein percentage, DIM = days in milk, BW = bodyweight (kg/cow), Age = age of the cows (years)

Equation	Variables and parameter estimates ± standard error	max_VIF	*det*{R}
	With DMI		
(1)	$F_{DM} = -0.576 \pm 0.222 + (0.370 \pm 0.006 \times DMI) + (-0.075 \pm 0.010 \times CP) + (0.059 \pm 0.006 \times ADF)$	1.02	0.90
(2)	$F_C = (0.169 \pm 0.003 \times DMI) + (-0.034 \pm 0.004 \times CP) + (0.027 \pm 0.003 \times ADF) + (-0.075 \pm 0.019 \times m\mathrm{Pr}\,t)$	1.04	0.87
(3)	$F_{NDF} = -0.864 \pm 0.172 + (0.217 \pm 0.004 \times DMI) + (0.035 \pm 0.003 \times NDF) + (-0.039 \pm 0.007 \times CP)$	1.01	0.86
(4)	$F_{ADF} = -1.272 \pm 0.084 + (0.125 \pm 0.003 \times DMI) + (0.061 \pm 0.003 \times ADF)$	1.00	0.99
(5)	$F_N = -0.0368 \pm 0.007 + (0.0096 \pm 0.000 \times DMI) + (0.0022 \pm 0.000 \times CP) + (0.0034 \pm 0.001 \times lignin) + (-0.000043 \pm 0.000010 \times BW)$	1.09	0.80
(6)	$F_{Water} = (1.987 \pm 0.034 \times DMI) + (0.348 \pm 0.032 \times ADF) + (-0.412 \pm 0.052 \times CP) + (-0.074 \pm 0.009 \times DM) + (-0.0057 \pm 0.0012 \times DIM)$	1.16	0.80
(7)	$U_E = -7.742 \pm 2.367 + (0.388 \pm 0.055 \times DMI) + (0.726 \pm 0.096 \times CP) + (2.066 \pm 0.421 \times m\mathrm{Pr}\,t$	1.05	0.94
(8)	$U_C = -0.1601 \pm 0.0169 + (0.0082 \pm 0.0005 \times DMI) + (0.0107 \pm 0.0008 \times CP) + (0.00013 \pm 0.00002 \times BW)$	1.13	0.84
(9)	$U_N = -0.2837 \pm 0.0135 + (0.0068 \pm 0.0004 \times DMI) + (0.0155 \pm 0.0006 \times CP) + (0.00013 \pm 0.00001 \times DIM) + (0.000092 \pm 0.000017 \times BW)$	1.34	0.66
	Without DMI		
(10)	$F_{DM} = 0.846 \pm 0.469 + (0.098 \pm 0.004 \times Milk) + (-0.097 \pm 0.021 \times CP) + (0.080 \pm 0.012 \times ADF) + (0.0038 \pm 0.0005 \times BW)$	1.04	0.80
(11)	$F_C = 0.468 \pm 0.232 + (0.046 \pm 0.002 \times Milk) + (-0.047 \pm 0.010 \times CP) + (0.037 \pm 0.006 \times ADF) + (0.0016 \pm 0.0002 \times BW)$	1.04	0.80
(12)	$F_{NDF} = (0.056 \pm 0.003 \times Milk) + (-0.059 \pm 0.010 \times CP) + (0.0435 \pm 0.0042 \times NDF) + (0.0023 \pm 0.0003 \times BW)$	1.00	0.77
(13)	$F_{ADF} = -0.973 \pm 0.152 + (0.0325 \pm 0.0016 \times Milk) + (0.0675 \pm 0.0043 \times ADF) + (0.0014 \pm 0.0002 \times BW)$	1.00	0.98
(14)	$F_N = (0.00245 \pm 0.00011 \times Milk) + (0.00643 \pm 0.00082 \times \mathrm{LIG}) + (0.000094 \pm 0.000009 \times BW)$	1.00	0.99
(15)	$F_{Water} = (0.559 \pm 0.025 \times Milk) + (0.521 \pm 0.060 \times ADF) + (0.569 \pm 0.100 \times CP) + (0.024 \pm 0.003 \times BW) + (-0.033 \pm 0.012 \times Age)$	1.17	0.66
(16)	$U_E = -0.644 \pm 0.226 + (0.778 \pm 0.099 \times CP) + (1.520 \pm 0.426 \times m\mathrm{Pr}\,t)$	1.00	0.99
(17)	$U_C = -0.1167 \pm 0.0201 + (0.0013 \pm 0.0002 \times Milk) + (0.0106 \pm 0.0009 \times CP) + (0.00024 \pm 0.00002 \times BW)$	1.03	0.87
(18)	$U_N = -0.2578 \pm 0.0183 + (0.0152 \pm 0.0007 \times CP) + (0.0132 \pm 0.0031 \times m\mathrm{Pr}\,t) + (0.00021 \pm 0.00002 \times BW)$	1.01	0.98

Table 1. Summary statistics for the data ($n = 1106$)

F_{Water}, F_{DM}, F_C, F_N, F_{NDF}, F_{ADF}, F_{HC} *and* F_{CL} = faecal water, dry matter (DM), carbon, nitrogen, neutral detergent fibre (NDF), acid detergent fibre (ADF), hemicellulose and cellulose outputs, respectively. U_E, U_C and U_N = total urine output, urinary carbon and nitrogen outputs, respectively. T_E, T_C, T_N, $R_{C:N}$ and C_{DM} = total fresh manure output, total carbon and nitrogen outputs, carbon to nitrogen ratio in fresh manure and dry matter concentration in fresh manure, respectively

Variable	Mean	s.d.	CV%	Minimum	Maximum
Independent or predictor variables					
Diet composition					
DM (% of diet)	68.0	20.0	29	30.2	93.8
CP (% of DM)	16.1	2.40	15	10.3	21.9
NDF (% of DM)	33.8	7.13	21	16.1	57.2
ADF (% of DM)	19.6	4.30	22	8.97	31.4
Lignin (% of DM)	4.33	1.48	34	1.26	8.44
Ether extract (% of DM)	2.56	0.75	29	0.52	4.95
Ash (% of DM)	6.31	1.11	18	3.54	9.99
Intake (kg/day)					
DM	15.6	4.08	26	6.40	28.7
N	0.41	0.13	32	0.14	0.93
NDF	5.31	1.81	34	1.15	12.0
ADF	3.08	1.06	35	0.70	6.82
Lignin	0.69	0.31	45	0.12	1.84
Production and other characteristics					
Milk yield (kg/day)	21.6	9.80	45	1.04	49.1
Milk fat (%)	3.50	0.76	22	1.30	7.60
Milk protein (%)	3.27	0.41	13	2.30	5.75
Age (years)	5.77	2.33	40	2.00	15.4
Bodyweight (kg/cow)	603	78.3	13	351	854
Days in milk	175	90.0	51	0.00	488
Response variables					
Faecal excretions (F_x, kg/day) and faecal C content (C_C, kg/kg of DM)					
F_{Water}	25.0	9.80	39	4.03	59.8
F_{DM}	5.20	1.77	34	1.18	10.7
F_C	2.40	0.80	33	0.54	4.76
F_N	0.13	0.04	31	0.05	0.25
F_{NDF}	3.06	1.04	34	0.54	7.21
F_{ADF}	1.91	0.65	34	0.34	4.24
F_{HC}	1.17	0.49	42	0.10	3.22
F_{CL}	1.16	0.42	36	0.21	2.76
C_C	0.46	0.02	04	0.38	0.52
Urinary excretions (U_x, kg/day)					
U_E	16.6	6.60	40	4.38	34.9
U_C	0.22	0.07	32	0.07	0.43
U_N	0.16	0.08	48	0.03	0.40
Total output (T_x, kg/day), C : N ratio ($R_{C:N}$), and DM content (C_{DM}, w/w) of fresh manure					
T_E	46.7	14.0	30	16.9	98.5
T_C	2.59	0.80	31	0.68	5.09
T_N	0.29	0.10	34	0.09	0.66
$R_{C:N}$	9.50	2.69	28	4.24	19.6
C_{DM}	0.11	0.02	17	0.05	0.19

At the herd level

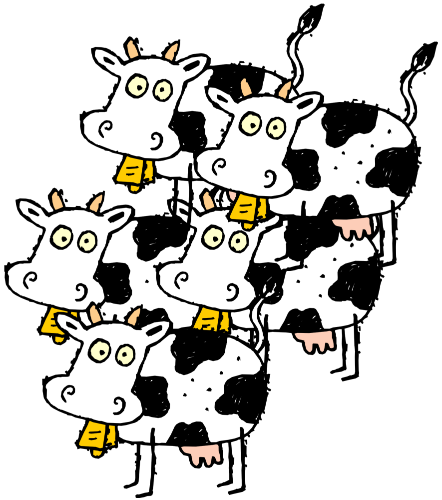

2023-04-17

Modelling livestock
└Models for cattle
  └Models for herds
    └At the herd level

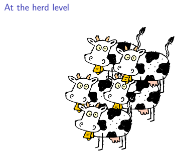

Physica D 240 (2011) 1497–1509

Contents lists available at SciVerse ScienceDirect

Physica D

journal homepage: www.elsevier.com/locate/physd

A mathematical model for the dynamics and synchronization of cows

Jie Sun [a,1], Erik M. Bollt [a], Mason A. Porter [b,c,*], Marian S. Dawkins [d]

[a] *Department of Mathematics, Clarkson University, Potsdam, NY 13699-5815, USA*

[b] *Mathematical Institute, University of Oxford, Oxford OX1 3LB, UK*

[c] *CABDyN Complexity Centre, University of Oxford, Oxford OX1 1HP, UK*

[d] *Department of Zoology, University of Oxford, OX1 3PS, UK*

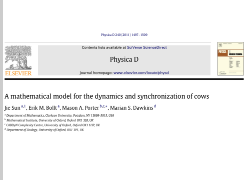

We model the biological status of a single cow by

$$w = (x, y; \theta) \in [0, 1] \times [0, 1] \times \Theta. \tag{1}$$

The real variables x and y represent, respectively, the extent of desire to eat and lie down of the cow, and

$$\theta \in \Theta = \{\mathcal{E}, \mathcal{R}, \mathcal{S}\} \tag{2}$$

is a discrete variable that represents the state of the cow (see the equations below for descriptions of the states). Throughout this paper, we will refer to θ as a *symbolic variable* or a *state variable*. One can think of the symbolic variable θ as describing a switch that triggers different time-evolution rules for the other two variables x and y.

We model the dynamics of a single cow in different states using

$$(\mathcal{E})\ \textit{Eating state:} \quad \begin{cases} \dot{x} = -\alpha_2 x, \\ \dot{y} = \beta_1 y. \end{cases} \tag{3}$$

$$(\mathcal{R})\ \textit{Resting state:} \quad \begin{cases} \dot{x} = \alpha_1 x, \\ \dot{y} = -\beta_2 y. \end{cases} \tag{4}$$

$$(\mathcal{S})\ \textit{Standing state:} \quad \begin{cases} \dot{x} = \alpha_1 x, \\ \dot{y} = \beta_1 y, \end{cases} \tag{5}$$

where the calligraphic letters inside parentheses indicate the corresponding values of θ. For biological reasons, the parameters α_1, α_2, β_1, and β_2 must all be positive real numbers. They can be interpreted as follows:

$$\begin{cases} \alpha_1 : \text{rate of increase of hunger,} \\ \alpha_2 : \text{decay rate of hunger,} \\ \beta_1 : \text{rate of increase of desire to lie down,} \\ \beta_2 : \text{decay rate of desire to lie down.} \end{cases}$$

2.2. *Switching conditions*

The dynamics within each state does not fully specify the equations governing a single cow. To close the bovine equations, we also need switching conditions that determine how the state variable θ changes. We illustrate these switching conditions in Fig. 1 and describe them in terms of equations as follows:

$$\theta \to \begin{cases} \mathcal{E} & \text{if } \theta \in \{\mathcal{R}, \mathcal{S}\} \text{ and } x = 1, \\ \mathcal{R} & \text{if } \theta \in \{\mathcal{E}, \mathcal{S}\} \text{ and } x < 1, y = 1, \\ \mathcal{S} & \text{if } \theta \in \{\mathcal{E}, \mathcal{R}\} \text{ and } x < 1, y = \delta \text{ (or } x = \delta, y < 1). \end{cases} \tag{6}$$

2.2. *Switching conditions*

The dynamics within each state does not fully specify the equations governing a single cow. To close the bovine equations, we also need switching conditions that determine how the state variable θ changes. We illustrate these switching conditions in Fig. 1 and describe them in terms of equations as follows:

$$\theta \to \begin{cases} \mathcal{E} & \text{if } \theta \in \{\mathcal{R}, \mathcal{S}\} \text{ and } x = 1, \\ \mathcal{R} & \text{if } \theta \in \{\mathcal{E}, \mathcal{S}\} \text{ and } x < 1, y = 1, \\ \mathcal{S} & \text{if } \theta \in \{\mathcal{E}, \mathcal{R}\} \text{ and } x < 1, y = \delta \text{ (or } x = \delta, y < 1). \end{cases} \tag{6}$$

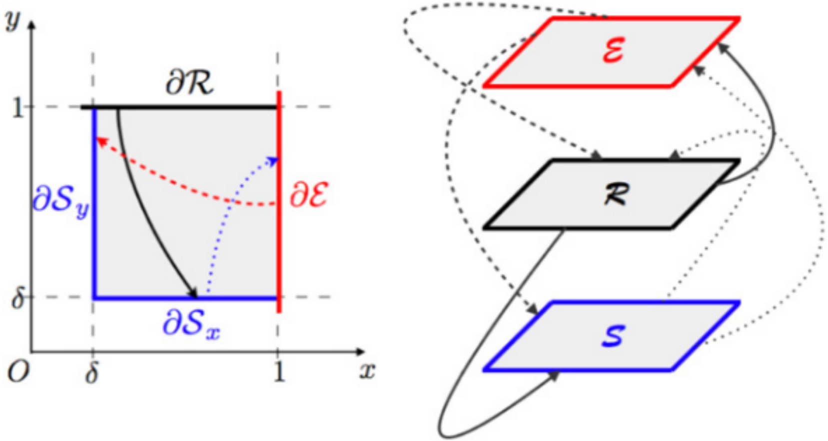

Fig. 1. (Color online) Switching conditions for the single-cow model. In the left panel, we project the set $[\delta, 1] \times [\delta, 1] \times \Theta$ onto $\mathbb{R}^2$, where edges of the square correspond to the borders at which switching occurs. In the right panel, we show the detailed switching situations; an arrow from one edge to another indicates the change of θ at that edge from one state to the other. (The arrows with solid curves are the ones that leave state $\mathcal{R}$, those with dashed curves are the ones that leave state $\mathcal{E}$, and those with dotted curves are the ones that leave state $\mathcal{S}$.)

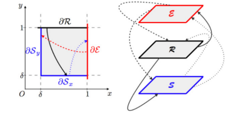

Fig. 1. (Color online) Switching conditions for the single-cow model. In the left panel, we project the set $[\delta, 1] \times [\delta, 1] \times \Theta$ onto $\mathbb{R}^2$, where edges of the square correspond to the borders at which switching occurs. In the right panel, we show the detailed switching situations; an arrow from one edge to another indicates the change of θ at that edge from one state to the other. (The arrows with solid curves are the ones that leave state $\mathcal{R}$, those with dashed curves are the ones that leave state $\mathcal{E}$, and those with dotted curves are the ones that leave state $\mathcal{S}$.)

4.1. The coupling scheme

There are numerous possible ways to model the coupling between cows. We have chosen one based on the hypothesis that a cow feels hungrier when it notices other cows eating and feels a greater desire to lie down when it notices other cows lying down. (We briefly discuss other possibilities in Section 5.) This provides a coupling that does not have a spatial component, in contrast to the agent-based approach of Ref. [30]. We therefore assume implicitly that space is unlimited, so we are considering cows to be in a field rather than in a pen. We suppose that the herd consists of n cows and use i to represent the ith cow in the herd. This yields herd equations given by

$$\begin{cases} \dot{x}_i = \left[\alpha^{(i)}(\theta_i) + \dfrac{\sigma_x}{k_i}\displaystyle\sum_{j=1}^{n} a_{ij}\chi_{\mathcal{E}}(\theta_j)\right]x_i, \\ \dot{y}_i = \left[\beta^{(i)}(\theta_i) + \dfrac{\sigma_y}{k_i}\displaystyle\sum_{j=1}^{n} a_{ij}\chi_{\mathcal{R}}(\theta_j)\right]y_i, \end{cases} \tag{26}$$

with the switching condition given by Eq. (6) for each individual cow. The summation terms in both equations give the coupling terms of this system. The matrix $A = [a_{ij}]_{n\times n}$ is a time-dependent adjacency matrix that represents the network of cows. Its components are given by

$$a_{ij}(t) = \begin{cases} 1 & \text{if the } i\text{th cow perceives the} \\ & j\text{th cow at time } t, \\ 0 & \text{if the } i\text{th cow does not perceive the} \\ & j\text{th cow at time } t. \end{cases} \tag{27}$$

Additionally, $k_i = \sum_{j=1}^{n} A_{ij}$ is the degree of node i (i.e., the number of cows to which it is connected), and the coupling strengths σ_x and σ_y are non-negative (and usually positive) real numbers. This is designed to emphasize that animal interaction strengths consider proximity to neighboring animals.

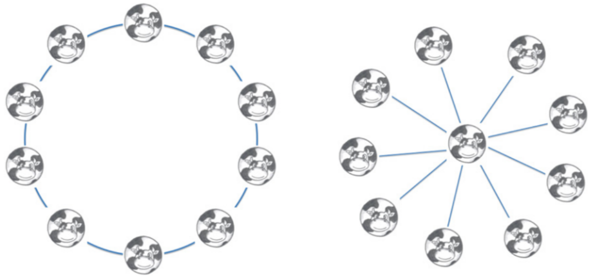

Fig. 8. (Color online) Example network architectures for coupled cows: (left) circular lattice with 10 nodes and (right) star graph with 10 nodes. (The spherical cow image was created for this paper by Yulian Ng and is used with her permission.)

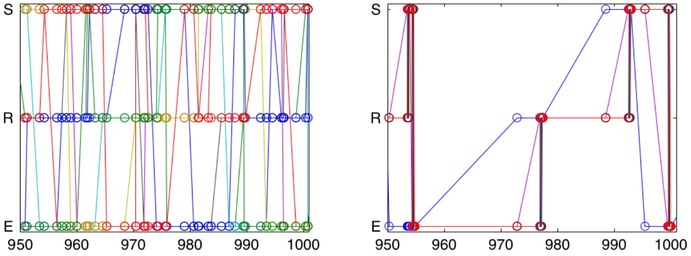

Fig. 9. (Color online) Typical state transitions for coupled cows in (left) a circular lattice and (right) a star graph with fixed coupling strengths $\sigma_x = \sigma_y = 0.05$. We plot (artificial) straight lines to help visualize transitions between states (which are represented by open circles, with different colors representing different cows). The horizontal axis is time. Some of the curves overlap (so that fewer than 10 colors are visible) due to the partial synchrony between individual cows.

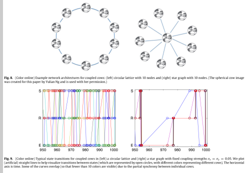

ELSEVIER
Ecological Modelling 119 (1999) 231–238
ECOLOGICAL MODELLING

Model for the spatial pattern formed by a small herd in grazing cattle

Masae Shiyomi [a,*], Mikinori Tsuiki [b]

[a] *Faculty of Science, Ibaraki University, Bunkyo 2-1-1, Mito 310-8512, Japan*
[b] *Faculty of Agriculture, Iwate University, Ueda 3-18-8, Morioka 020-0066, Japan*

Accepted 25 February 1999

ELSEVIER Ecological Modelling 119 (1999) 231–238 ECOLOGICAL MODELLING
Model for the spatial pattern formed by a small herd in grazing cattle
Masae Shiyomi [a,*], Mikinori Tsuiki [b]
[a] Faculty of Science, Ibaraki University, Bunkyo 2-1-1, Mito 310-8512, Japan
[b] Faculty of Agriculture, Iwate University, Ueda 3-18-8, Morioka 020-0066, Japan
Accepted 25 February 1999

increase. In other words, the area reaches an equilibrium, and attraction activities (desire to be in a group) and repulsion activities (maintenance of individual space) operating among individuals are well-balanced in the herd although the area they occupy is elastic within fences. Because the area they occupy indicates the strength of unity or closeness among individuals in the herd, the analysis of the area should provide basic information for managing a cattle herd in paddocks. In the present study, only the distance between the far-left and far-right individuals in a small herd grazed in an experimental strip-wise pasture was observed instead of the area the cattle herd occupied. This distance is referred to as 'troop length' thereafter.

increase. In other words, the area reaches an equilibrium, and attraction activities (desire to be in a group) and repulsion activities (maintenance of individual space) operating among individuals are well-balanced in the herd although the area they occupy is elastic within fences. Because the area they occupy indicates the strength of unity or closeness among individuals in the herd, the analysis of the area should provide basic information for managing a cattle herd in paddocks. In the present study, only the distance between the far-left and far-right individuals in a small herd grazed in an experimental strip-wise pasture was observed instead of the area the cattle herd occupied. This distance is referred to as 'troop length' thereafter.

Suppose that there is a straight line with length of θ, and n individuals are located independently and randomly at points whose distances from the origin are x_1, x_2,. . . , x_n according to the following rectangular distribution:

$$f(x)\,\mathrm{d}x = \mathrm{d}x/\theta \quad \text{for} \quad 0 \le x \le \theta$$

$$f(x)\,\mathrm{d}x = 0 \text{ elsewhere.} \tag{1}$$

Suppose that there is a straight line with length of θ, and n individuals are located independently and randomly at points whose distances from the origin are x_1, x_2,. . . , x_n according to the following rectangular distribution:

$$f(x)\,\mathrm{d}x = \mathrm{d}x/\theta \quad \text{for} \quad 0 \le x \le \theta$$

$$f(x)\,\mathrm{d}x = 0 \text{ elsewhere.} \tag{1}$$

2.1. *Probability density function of the troop length in the case of random patterns*

We assume that the n independent individuals are located randomly on the line segment with a length of θ, and let y be the 'troop length'. The probability density function for the troop length was derived using a sampling theory of order statistics (e.g. Wilks, 1962), in the following form:

$$f(y)\,\mathrm{d}y = n(n-1)y^{n-2}(\theta - y)/\theta^n \mathrm{d}y \quad \text{for} \quad 0 \leq x \leq \theta$$

$$f(y)\,\mathrm{d}y = 0 \text{ elsewhere.} \qquad (2)$$

The expected distance, μ, and the variance, σ^2, for y are expressed by the following equations, respectively: $\mu = (n-1)\theta/(n+1)$ and $\sigma^2 = 2(n-1)\theta^2/\{(n+2)(n+1)^2\}$.

2.1. *Probability density function of the troop length in the case of random patterns*

We assume that the n independent individuals are located randomly on the line segment with a length of θ, and let y be the 'troop length'. The probability density function for the troop length was derived using a sampling theory of order statistics (e.g. Wilks, 1962), in the following form:

$f(y)\,\mathrm{d}y = n(n-1)y^{n-2}(\theta - y)/\theta^n \mathrm{d}y$ for $0 \leq x \leq \theta$

$f(y)\,\mathrm{d}y = 0$ elsewhere. (2)

The expected distance, μ, and the variance, σ^2, for y are expressed by the following equations, respectively: $\mu = (n-1)\theta/(n+1)$ and $\sigma^2 = 2(n-1)\theta^2/\{(n+2)(n+1)^2\}$.

2.2. Deterministic model describing the changes in troop length

We express the troop length at time t by y, and assume that y changes during an infinitesimal period of time, dt, according to the following relationship (Fig. 1):

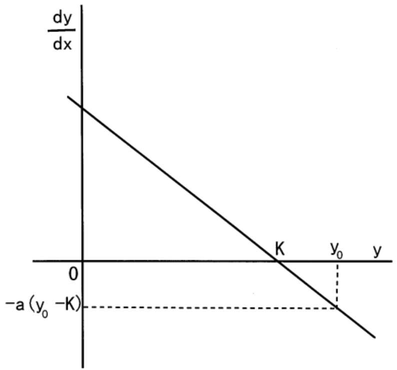

Fig. 1. Deterministic model representing the relationship between the troop length, y, and the change in an infinitesimal time period, dy/dt.

$$dy/dt = -a(y - K), \; a \geq 0, \; K \geq 0, \tag{3}$$

where a indicates the 'convergence rate' of troop length to the 'equilibrium' troop length K. Eq. (3) indicates that: (1) troop length, y, decreases during the following dt if $y > K$ (attraction); (2) y increases during the following dt if $y < K$ (repulsion); and (3) y does not change during the following dt if $y = K$ (equilibrium). Eq. (3) implies that the changes in the troop length with time occur solely based on attraction and repulsion operating among individuals within the herd. When we assume that the troop length at time t_0 is y_0, the following solution is obtained from Eq. (3):

$$y = K - (K - y_0)\, e^{-at}. \tag{4}$$

For $t \to \infty$, the troop length, y, in Eq. (4) approaches K in monotone. It is empirically evident that this deterministic model does not fit to the actual behavior of a cattle herd because it is unlikely that the troop length of cattle converges to a constant, K, with time, without fluctuations. Actual troop length may fluctuate around K as the example shown below (Fig. 3). A stochastic model modifying Eq. (3) to describe the actual fluctuations is proposed in the following sections.

$$dy/dt = -a(y - K), \; a \geq 0, \; K \geq 0, \tag{3}$$

where a indicates the 'convergence rate' of troop length to the 'equilibrium' troop length K. Eq. (3) indicates that: (1) troop length, y, decreases during the following dt if $y > K$ (attraction); (2) y increases during the following dt if $y < K$ (repulsion); and (3) y does not change during the following dt if $y = K$ (equilibrium). Eq. (3) implies that the changes in the troop length with time occur solely based on attraction and repulsion operating among individuals within the herd. When we assume that the troop length at time t_0 is y_0, the following solution is obtained from Eq. (3):

$$y = K - (K - y_0)\, e^{-at}. \tag{4}$$

For $t \to \infty$, the troop length, y, in Eq. (4) approaches K in monotone. It is empirically evident that this deterministic model does not fit to the actual behavior of a cattle herd because it is unlikely that the troop length of cattle converges to a constant, K, with time, without fluctuations. Actual troop length may fluctuate around K as the example shown below (Fig. 3). A stochastic model modifying Eq. (3) to describe the actual fluctuations is proposed in the following sections.

2.3. Stochastic model describing changes in troop length

We assume that $\mathrm{d}y/\mathrm{d}t$ follows: (1) the attractive and repulsive activities operating between individuals; and (2) a random movement or involuntary activity referred to as white noise in physics, ε, in the changes of the troop length at time t. Then, we have

$$\mathrm{d}y/\mathrm{d}t = -a(y-K)+\varepsilon. \tag{5}$$

Let us assume that the probability that the troop length, y, occurs between Y and $Y+\Delta Y$ at t, where ΔY denotes an infinitesimal length, is expressed by $g(y,t)\,\mathrm{d}y$:

$$\mathrm{Prob}\{Y \le y(t) \le Y+\Delta Y\} = g(y,t)\,\mathrm{d}y,$$

where g denotes a probability density function of y at t.

2.3. Stochastic model describing changes in troop length

We assume that dy/dt follows: (1) the attractive and repulsive activities operating between individuals; and (2) a random movement or involuntary activity referred to as white noise in physics, ε, in the changes of the troop length at time t. Then, we have

dy/dt = −a(y − K) + ε. (5)

Let us assume that the probability that the troop length, y, occurs between Y and Y + ΔY at t, where ΔY denotes an infinitesimal length, is expressed by g(y, t) dy:

Prob{Y ≤ y(t) ≤ Y + ΔY} = g(y, t) dy,

where g denotes a probability density function of y at t.

Then, by applying the Kolmogorov diffusion equation (e.g. Bharucha-Reid, 1960) to Eq. (5), we obtain the following equation:

$$\frac{\partial g(y,t)}{\partial t} = \frac{-\partial}{\partial y}[-a(y-K)g(y,t)] + \frac{1}{2}\frac{\partial^2}{\partial y^2}[\sigma^2 g(y,t)], \tag{6}$$

where σ^2 denotes a constant relating to the intensity of the involuntary activity.

Then, by applying the Kolmogorov diffusion equation (e.g. Bharucha-Reid, 1960) to Eq. (5), we obtain the following equation:

$$\frac{\partial g(y,t)}{\partial t} = \frac{-\partial}{\partial y}[-a(y-K)g(y,t)] + \frac{1}{2}\frac{\partial^2}{\partial y^2}[\sigma^2 g(y,t)], \tag{6}$$

where σ^2 denotes a constant relating to the intensity of the involuntary activity.

In a pasture in which a given cattle herd is grazed for a long period of time, the interrelationships between the herd members and the troop length of the herd are likely to be stable. We do not need to solve Eq. (6) directly, because of this stability, and we obtain a probability density function of y, only by putting $\partial g(y,\ t)/\partial t = 0$. Then, we have:

$$a(y-K)g(y)+\frac{1}{2}\frac{\mathrm{d}}{\mathrm{d}y}[\sigma^2 g(y)]=0, \tag{7}$$

where $g(y)$ is independent of t.

From Eq. (7), we obtain the probability density function, $g(y)$, for troop length, y, as follows:

$$g(y)=\exp\left[-\frac{a}{\sigma^2}(y-K)^2\right]\Big/R,$$

where

$$R=\int_0^{\theta}\exp\left[-\frac{a}{\sigma^2}(y-k)^2\right]\mathrm{d}\,y,\ \ a\geq 0,\ \ 0\leq K\leq\theta \tag{8}$$

In a pasture in which a given cattle herd is grazed for a long period of time, the interrelationships between the herd members and the troop length of the herd are likely to be stable. We do not need to solve Eq. (6) directly, because of this stability, and we obtain a probability density function of y, only by putting $\partial g(y,\ t)/\partial t = 0$. Then, we have:

$$a(y-K)g(y)+\frac{1}{2}\frac{\mathrm{d}}{\mathrm{d}y}[\sigma^2 g(y)]=0, \tag{7}$$

where $g(y)$ is independent of t.

From Eq. (7), we obtain the probability density function, $g(y)$, for troop length, y, as follows:

$$g(y)=\exp\left[-\frac{a}{\sigma^2}(y-K)^2\right]\Big/R,$$

where

$$R=\int_0^{\theta}\exp\left[-\frac{a}{\sigma^2}(y-k)^2\right]\mathrm{d}\,y,\ \ a\geq 0,\ \ 0\leq K\leq\theta \tag{8}$$

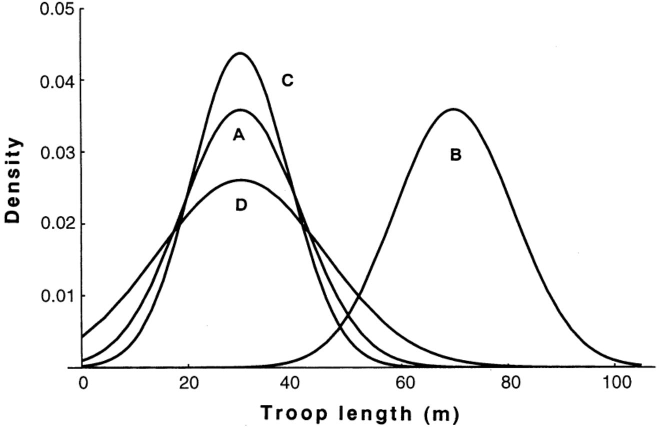

Fig. 2. Examples for various values of three parameters in Eq. (8) ($\theta = 100$). (A) $K = 30$, $a = 1.0$, $\sigma^2 = 250$; (B) $K = 70$, $a = 1.0$, $\sigma^2 = 250$; (C) $K = 30$, $a = 1.5$, $\sigma^2 = 250$; and (D) $K = 30$, $a = 1.0$, $\sigma^2 = 500$.

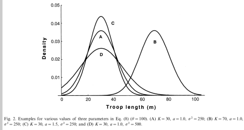

3.1. Materials and methods

A pasture 88 m × 6 m in size was designed, to observe easily the cattle activities and to facilitate theoretical considerations under the experimental conditions, at the National Grassland Research Institute at Nishinasuno, Tochigi, Japan. The main plant species in the pasture were orchard grass, tall fescue and white clover. A grazing experiment was carried out using six Holstein heifers aged 1–2 years with a body weight ranging from 200 to 300 kg in 1979. The width of the pasture, 6 m, was sufficient for three or more cows to walk side by side. The positions of each of the six cows were visually observed and recorded every 20 min. The observation was started at 07:30 h on 5 June, and continued for ≈ 3 days except during the night when the positions could not be observed visually.

3.1. Materials and methods

A pasture 88 m × 6 m in size was designed, to observe easily the cattle activities and to facilitate theoretical considerations under the experimental conditions, at the National Grassland Research Institute at Nishinasuno, Tochigi, Japan. The main plant species in the pasture were orchard grass, tall fescue and white clover. A grazing experiment was carried out using six Holstein heifers aged 1–2 years with a body weight ranging from 200 to 300 kg in 1979. The width of the pasture, 6 m, was sufficient for three or more cows to walk side by side. The positions of each of the six cows were visually observed and recorded every 20 min. The observation was started at 07:30 h on 5 June, and continued for ≈ 3 days except during the night when the positions could not be observed visually.

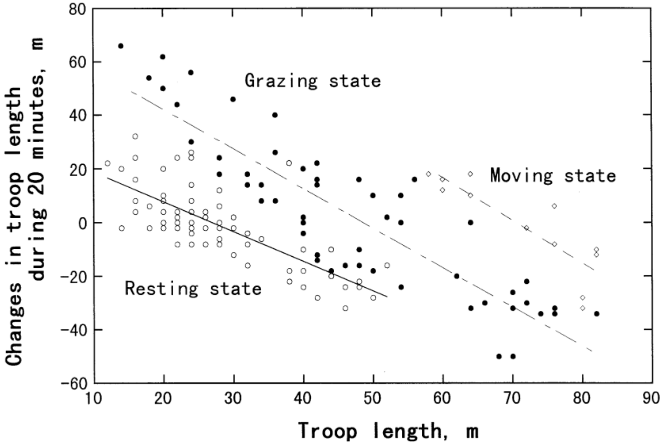

Fig. 3. Relationships, obtained in a field experiment, between the troop length at time t and change during successive 20 min intervals. Symbols ●, × and ○ denote the resting, feeding and moving states, respectively.

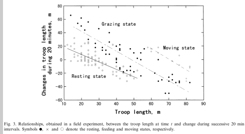

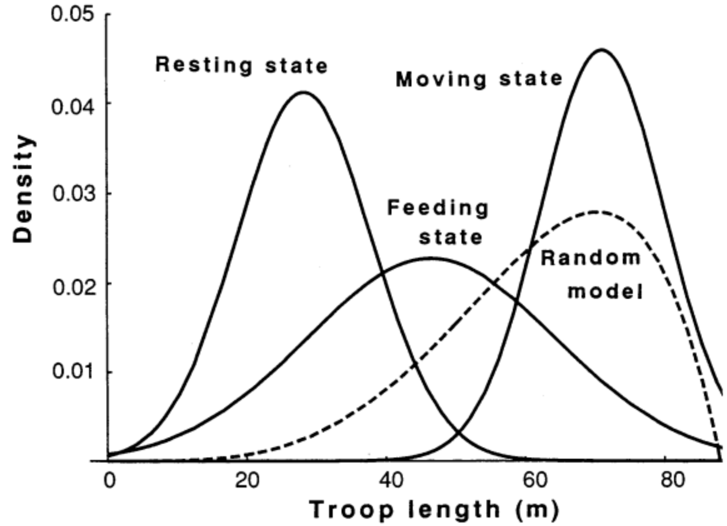

Fig. 4. Probability density functions, obtained for the experimental data, for the resting, feeding and moving states (Eq. (8)) and for the hypothetical random spatial pattern (Eq. 2). The parameter values used in the calculations are listed in Table 1.

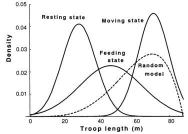

Fig. 4. Probability density functions, obtained for the experimental data, for the resting, feeding and moving states (Eq. (8)) and for the hypothetical random spatial pattern (Eq. 2). The parameter values used in the calculations are listed in Table 1.

Published 1989

4 Measurements of the Plant-Animal Interface in Grazing Research[1]

S. W. Coleman

USDA-ARS
Forage and Livestock Research Laboratory
El Reno, Oklahoma

T. D. A. Forbes

Texas A&M University
Uvalde, Texas

J. W. Stuth

Texas A&M University
College Station, Texas

Published 1989
4 Measurements of the Plant-Animal Interface in Grazing Research[1]
S. W. Coleman
USDA-ARS
Forage and Livestock Research Laboratory
El Reno, Oklahoma
T. D. A. Forbes
Texas A&M University
Uvalde, Texas
J. W. Stuth
Texas A&M University
College Station, Texas

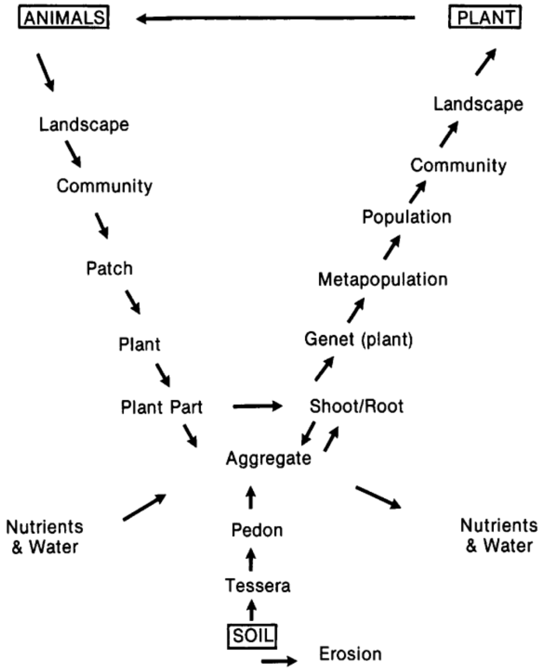

The hierarchical context of the plant-animal interface.

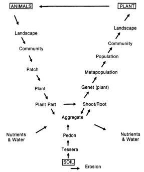
The hierarchical context of the plant-animal interface.

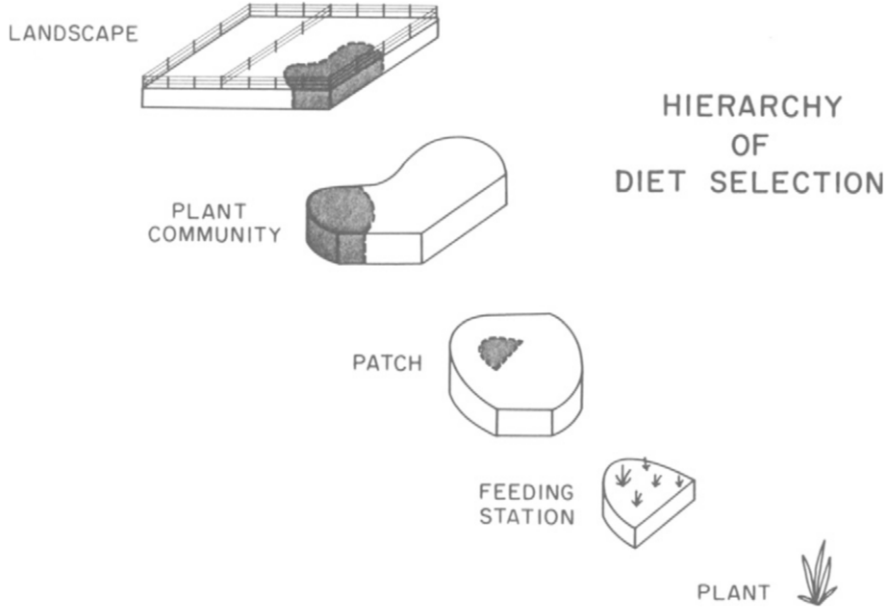

Fig. 4–2. The hierarchical context of diet selection as it descends from the landscape to the individual plant.

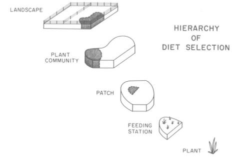
Fig. 4–2. The hierarchical context of diet selection as it descends from the landscape to the individual plant.

Ecological Modelling 270 (2013) 11–29

Contents lists available at ScienceDirect

Ecological Modelling

journal homepage: www.elsevier.com/locate/ecolmodel

A model of diurnal grazing patterns and herbage intake of a dairy cow, MINDY: Model description

Pablo Gregorini[a,*], Pierre C. Beukes[a], Alvaro J. Romera[a], Gil Levy[a], Mark D. Hanigan[b]

[a] DairyNZ, Ltd., Private Bag 3221, Hamilton, New Zealand
[b] Virginia Polytechnic Institute and State University, Blacksburg, VA 24061, USA

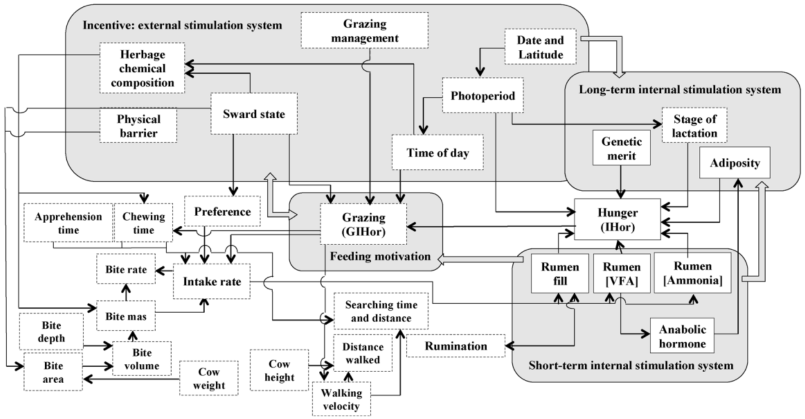

Fig. 1. Schematic representation of MINDY: a mechanistic and dynamic model to simulate diurnal patterns of herbage intake and grazing behavior of a grazing dairy cow. White boxes with solid lines represent true pools (hard components) of the model, white dashed with dashed lines represent soft components of the model, solid arrows represent modifiers. Grey boxes (functional components) and arrows represent the motivational system of feeding behavior adapted from Jensen and Toates (1993), Hughes and Duncan (1988) and Smith (1996).

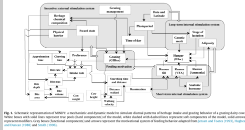

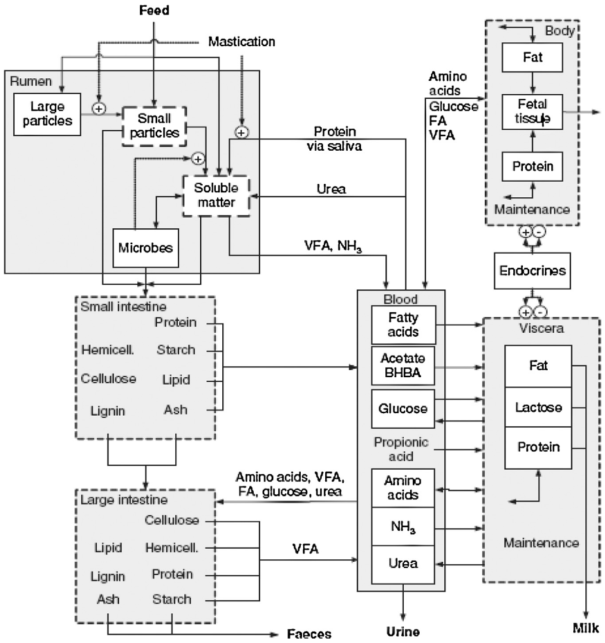

Fig. 2. A simplified schematic representation of Baldwin (1995). Adapted from Hanigan et al. (2008). Boxes with dashes lines represent conceptual compartments as defined in the model; boxes with solid lines represent pools; solid arrows represent modifiers; and the circles associated with dashed arrows indicate the direction of the modifies. FA, fatty acids, VFA, volatile fatty acids.

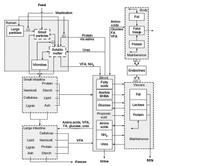

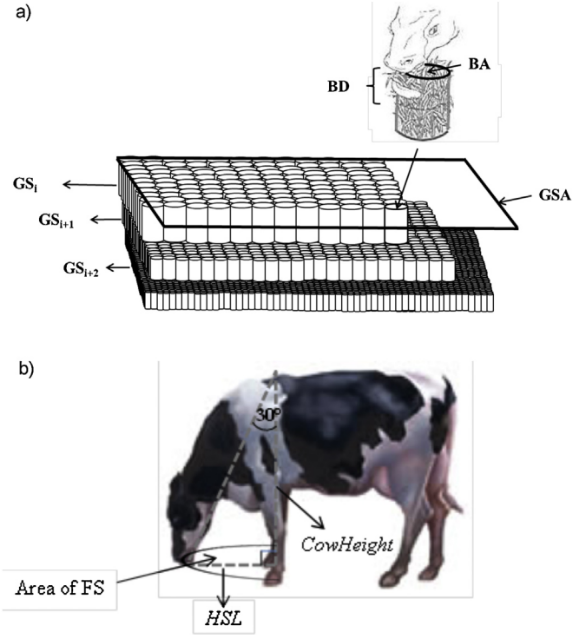

Fig. 3. a) A schematic representation of the bite features and grazing strata during grazing; b) a schematic representation of the harvesting step length calculus. (Adapted from Galli et al. (1999) and Baumont et al. (2004)).

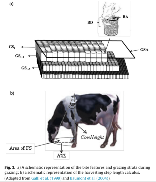

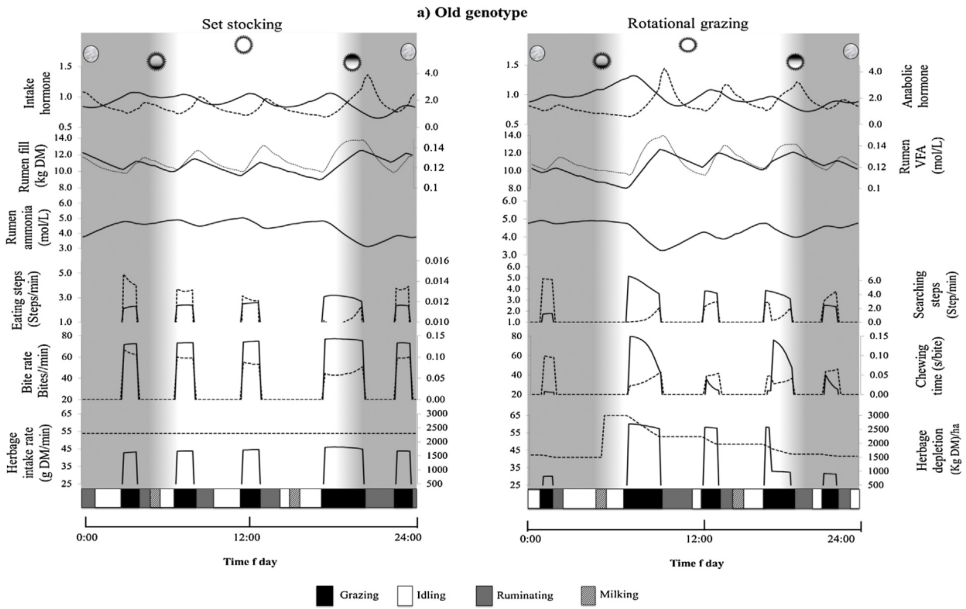

a) Old genotype
Set stocking
Rotational grazing
Intake hormone
Anabolic hormone
Rumen fill (kg DM)
Rumen VFA (mol/L)
Rumen ammonia (mol/L)
Eating steps (Steps/min)
Searching steps (Step/min)
Bite rate Bites/min)
Chewing time (s/bite)
Herbage intake rate (g DM/min)
Herbage depletion (Kg DM)/ha
0:00
12:00
24:00
Time f day
Grazing
Idling
Ruminating
Milking

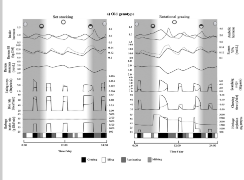

Model variables definitions and units.

Symbol	Definition	Value/Unit
ACHT	Actual chewing time	Days
ActualIR	Actual herbage intake rate of the grazing stratum *i*	kg/min
AHM	Available herbage mass modulator	Unitless
AHor	Anabolic hormone	Unitless
Am	Ruminal ammonia concentration	mmol/L
AmCor	Ruminal ammonia correction factor	Unitless
BA_i	Bite area of the grazing stratum *i*	m^2
BCS	Body condition score	Points
BCS_{Target}	Body condition score target	Points
BD_i	Bite depth of the grazing stratum *i*	m
BM_i	Bite mass of the grazing stratum *i*	kg
BR	Bite rata	Bites/day
Chewingfactor	Motivation to chew	Unitless
CowHeight	Animals height to the shoulder	m
CR_i	Consumption rate area of grazing stratum *i*	m^2/day
CurrentStratum	Upper stratum from the pair strata currently being grazed	
$CurrentStratum_{-1}$	Lower stratum from the pair strata currently being grazed	
C_{VFA}	Ruminal concentration of volatile fatty acids	mmol/L
DA	Dental arcade	m
Dailydistancewalked	Daily distance walked	m
DaylengthP1	Daylength excluding twilight hours for lactation module	
Daylight	Value representing light intensity	Unitless
DayTwlength	Length of the day including twilight hours	Days
DayTwlengthP2	Daylength including twilight hours	Days
DD	Defoliation depth	Proportion
DWH	Distance walked while harvesting	m
eLMI	Shape factor	Unitless
ETH_i	Extended tiller height of the grazing stratum *i*	m
ETH_{ini}	Initial extended tiller height	m
$ETHl_{im}$	Physical barrier under what cows are not allowed to or are not capable to graze	m
$F_{adjustment}$	Adjustment factor to the herbage chemical composition	Unitless
FdRat	Herbage intake rate	kg/day
FSR	Number of feeding stations per unit of time	FS/day
$GA_{CurrentStratum}$	Area harvested at the upper grazing stratum from the pair of grazing strata being grazed at the time	m^2
$GA_{CurrentStratum-1}$	Area harvested at the lower grazing stratum from the pair of grazing strata being grazed at the time	cm^2
GA_i	Rates of changes in GSA_i due to herbage consumption in grazing stratum *i*	m^2/day
GIHor	Motivation to graze	Unitless
GrazingSw	Switch to turn on and off grazing	Unitless
HDMI	Daily herbage dry matter intake	kg/day
HGR	Herbage growth rate	m/day
Hi	Median point height of each grazing stratum *i*	m
HighChewingMot	Constant	1, unitless, 31
HM	Herbage mass	kg/m^2
$HM_{totalavail}$	Sum of the herbage mass remaining in each grazing stratum	kg
$HM_{unavail}$	Unavailable herbage mass	kg
HSL	Length of a step while harvesting	m
iHM_{total}	Pre-grazing herbage mass	kg
$iHM_{totalavail}$	Pre-grazing available herbage mass	kg
IHor	Hunger hormone	Unitless
IHorCor	Scalar	1.0, unitless
IHorDeg	Intake hormone degradation	Unitless
IHorRange	Constant, Range of *IHor*	0.02, unitless
IHorSyn	Intake hormone synthesis	Unitless
iIHor	Initial IHor	1.0, unitless
k_{aHor}	Scalar	1.0, unitless
k_{Am}	Scalar	0.75, unitless
$k_{Chewfactor}$	Scalar	Unitless
k_{FdRat}	Function adjusting for adiposity and genetic potential	Unitless
kIHor	Constant	6.037, unitless
$k_{MamCells}$	Scalar (it scales *FdRat* with genetic potential)	0.1, unitless
k_{LPSP}	Rate of particle breakdown while ruminating	Unitless
k_{mPref}	Scalar to correct $PIR(i-1)/PIR(i)$ to achieve a proper curve shape	Unitless
k_{RumDM}	Scalar	9.5, unitless
k_{VFA}	Scalar	0.11, unitless
LagDMI	Intake lag function	Unitless
LateFeeding	Adjusting variable to reduce *MinIHor*	Days
LM	Linear masses of lamina	kg/m
LMI_i	Linear mass index of each grazing stratum *i*	Unitless
LowChewingMot	Constant	0.15, unitless
LP	Large particle size pool in the rumen	kg
MamCellPart	Number of milk secretor cells in the udder	Unitless
MBD_i	Mean bulk density of the grazing stratum *i*	kg/m^3
MBD_{sward}	Mean bulk density of the sward	kg/m^3
MeanLM	Mean linear mass of the tiller	kg/m
MeanSwHeight	Half of the ETHini	m

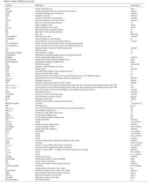

Table A.1 (*Continued*)

Symbol	Definition	Value/Unit
minimunGSA	Area threshold at which hrazing strating has '0' preference	m^2
MinLPRumntn	Minimum LP size required to initiate a ruination bout	kg
MSH	Momentary speed of harvesting	m/d
NightMealInter	Length of the last meal of the day	0.1, unitless
NightMealTime	Interval of the last meal of the day and the next meal during the night	0.044, unitless
Nstrata	Number of sward canopy accessible grazing strata	
$Nutrient_{adjustment}$	Adjustment factor to the herbage nutrients	Unitless
PCHT	Potential chewing time	Days
$PIR_{Current\ stratum}$	Potential intake rate in the upper stratum from the pair strata currently being grazed	kg/day
$PIR_{Current\ stratum+1}$	Potential intake rate in the lower stratum from the pair strata currently being grazed	kg/day
PIR_i	Potential herbage dry matter intake rate of the grazing stratum i	kg/day
$PREF_{CurrentStratum}$	Partial preference for the upper stratum from the pair strata currently being grazed	Unitless
$PREF_{inter}$	Constant to affect the intercept of the curve of partial preference for current currently being grazed	Unitless
pSTI	Momentary average proportion of time searching	Unitless
PT	Prehension time	Days
Rest	Resting (idling) time	Days
RumDM	Ruminal dry matter load	kg DM
Rumntn	Rumination time	Days
SDI	Distance walked while searching	m
SGR	Sward growth rate	m^2/d
SM	Linear masses of sheath	kg/m
SSpeedS	Momentary average speed while searching	m/day
SSR	Searching step rate	Searching steps/day
StartIHor	Constant, trigger point for starting a grazing bout	Unitless
STI	Searching time	Days
StopIHor	Constant, trigger point for ending a meal	Unitless
T	Time of day	Days
TA	Total area offered	m^2
TB_i	Time per bite at the grazing stratum i	Days
$Vm_{IHorSyn}$	Maximum velocity of *IHor* synthesis	Unitless
xaHor	Scalar	1.0, unitless
xAm	Scalar	1.12, unitless
xFdRatLag	Scalar (it rescales Roseler et al. (1997) lag function)	0.25, unitless
xRumDM	Scalar	1.0, unitless
xVFA	Scalar	10.0, unitless

Available online at www.sciencedirect.com

SCIENCE DIRECT®

ELSEVIER

Bioresource Technology 87 (2003) 113–124

BIORESOURCE TECHNOLOGY

Mathematical modeling of non-ideal mixing continuous flow reactors for anaerobic digestion of cattle manure

A. Keshtkar [a,b], B. Meyssami [b,*], G. Abolhamd [b], H. Ghaforian [a], M. Khalagi Asadi [a]

[a] *Center of Renewable Energies for Research and Application, Atomic Energy Organization of Iran, Tehran, Iran*

[b] *Faculty of Engineering, Department of Chemical Engineering, Tehran University, P.O. Box 11365-4563, Tehran, Iran*

Received 6 August 2001; received in revised form 14 January 2002; accepted 23 April 2002

Mathematical modeling of non-ideal mixing continuous flow reactors for anaerobic digestion of cattle manure

A. Keshtkar [a,b], B. Meyssami [b,*], G. Abolhamd [b], H. Ghaforian [a], M. Khalagi Asadi [a]

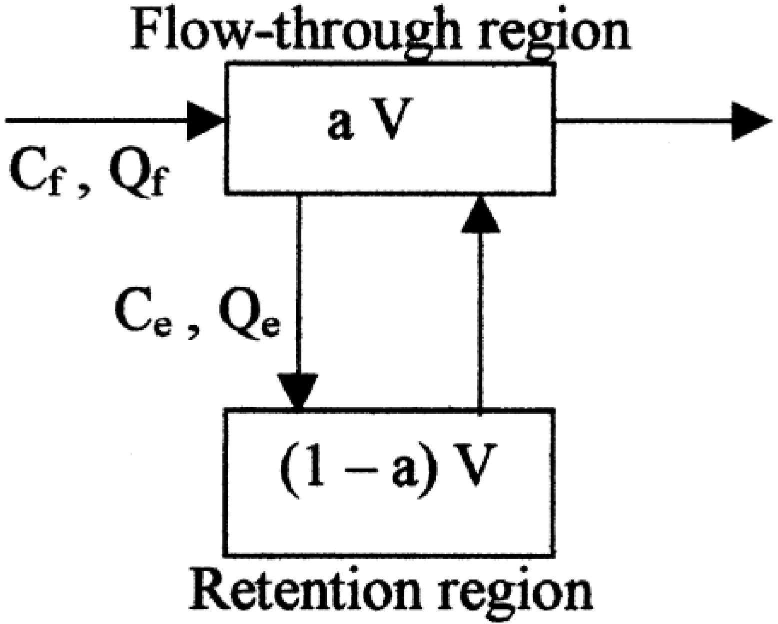

Fig. 1. Two-region mixing model.

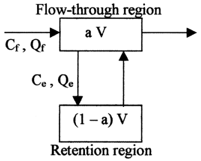

Fig. 1. Two-region mixing model.

$$
\begin{aligned}
(\mathrm{C_6H_{10}O_5} \cdot n\mathrm{NH_3})_{\mathrm{is}} \rightarrow\ & y_{\mathrm{e}}(\mathrm{C_6H_{10}O_5})_{\mathrm{s}} \\
& + (1 - y_{\mathrm{e}})(\mathrm{C_6H_{10}O_5} \cdot m\mathrm{NH_3})_{\mathrm{is}} \\
& + (n - (1 - y_{\mathrm{e}})m)\mathrm{NH_3}
\end{aligned} \tag{1}
$$

$$
\begin{aligned}
(\mathrm{C_6H_{10}O_5})_{\mathrm{s}} + 0.1115\,\mathrm{NH_3} \rightarrow\ & 0.1115\,\mathrm{C_5H_7NO_2} \\
& + 0.744\,\mathrm{CH_3COOH} \\
& + 0.5\,\mathrm{CH_3CH_2COOH} \\
& + 0.4409\,\mathrm{CH_3(CH_2)_2COOH} \\
& + 0.6909\,\mathrm{CO_2} + 0.0254\,\mathrm{H_2O}
\end{aligned} \tag{2}
$$

$$
\begin{aligned}
& \mathrm{CH_3CH_2COOH} + 0.06198\,\mathrm{NH_3} + 0.314\,\mathrm{H_2O} \\
& \quad \rightarrow 0.06198\,\mathrm{C_5H_7NO_2} + 0.9345\,\mathrm{CH_3COOH} \\
& \qquad + 0.6604\,\mathrm{CH_4} + 0.1607\,\mathrm{CO_2}
\end{aligned} \tag{3}
$$

$$
\begin{aligned}
& \mathrm{CH_3(CH_2)_2COOH} + 0.0653\,\mathrm{NH_3} + 0.5543\,\mathrm{CO_2} \\
& \quad + 0.5543\,\mathrm{H_2O} \rightarrow 0.0653\,\mathrm{C_5H_7NO_2} \\
& \quad + 1.8909\,\mathrm{CH_3COOH} + 0.4452\,\mathrm{CH_4}
\end{aligned} \tag{4}
$$

$$
\begin{aligned}
\mathrm{CH_3COOH} + 0.022\,\mathrm{NH_3} \rightarrow\ & 0.022\,\mathrm{C_5H_7NO_2} \\
& + 0.945\,\mathrm{CH_4} \\
& + 0.945\,\mathrm{CO_2} \\
& + 0.066\,\mathrm{H_2O}
\end{aligned} \tag{5}
$$

Nomenclature

a	mixing parameter
b	mixing parameter
C	liquid concentration, g/l
$[CO_2]$	free CO_2 in liquid concentration, mol/l
f	individual bacterial fraction in initial total biomass
f_{pr}	mass conversion factor of propionate to acetate = 0.8108
f_{but}	mass conversion factor of butyrate to acetate = 0.6818
F_t	biogas transfer rate, mol/d
$F(pH)$	pH function
H	Henry's constant, atm l/mol
HRT	hydraulic retention time
SRT	sludge retention time
k	hydrolysis rate constant, d^{-1}
K_0	non-inhibited hydrolysis rate constant, d^{-1}
K_a	dissociation constant
k_d	bacterial decay rate constant, d^{-1}
K_i	inhibition constant, g/l
K_s	Monod saturation constant, g/l
m	feed constant used in Eq. (1)
n	feed constant used in Eq. (1)
N	gas transfer rate, g/d
$[NH_3]$	free NH_3 in liquid concentration, mol/l
P	pressure, atm
pK_h	constant used in Eq. (16)
pK_l	constant used in Eq. (16)
Q	volumetric flow rate, d^{-1}
r_d	bacterial decay rate, g/l d
r_h	hydrolysis reaction rate, g/l d
r_s	substrate consumption rate, g/l d
r_x	bacterial growth rate, g/l d
R	gas constant, atm l/mol K
t	time, d
T	temperature, K
V_g	gas volume of reactor, l
V_l	liquid volume of reactor, l
VFA	volatile fatty acids
X	microorganisms concentration, g/l
y_e	yield factor used in Eq. (10)
α	flow-through region
β	retention region
θ	HRT, d
μ	specific growth rate, d^{-1}
μ_{max}	maximum specific growth rate, d^{-1}

Subscripts

ac	acetate
am	ammonia
A	acidogenic bacteria
AB	butyric degrading acetogenic bacteria
AP	propionate degrading acetogenic bacteria
but	butyrate
c	carbon dioxide
e	exchange between zones
f	feed
i	component i
is	insoluble substrate
m	methane
M	methanogenic bacteria
pr	propionate
s	soluble substrate
t	total
w	water

Ionic dissociation equations

$$CO_2 + H_2O \leftrightarrow HCO_3^- + H^+ \quad k_{a1} = \frac{[HCO_3^-][H^+]}{[CO_2]} \tag{A.25}$$

$$HCO_3^- \leftrightarrow CO_3^{2-} + H^+ \quad k_{a2} = \frac{[CO_3^{2-}][H^+]}{[HCO_3^-]} \tag{A.26}$$

$$HAc \leftrightarrow Ac^- + H^+ \quad k_{a3} = \frac{[AC^-][H^+]}{[HAc]} \tag{A.27}$$

$$HPr \leftrightarrow Pr^- + H^+ \quad k_{a4} = \frac{[Pr^-][H^+]}{[HPr]} \tag{A.28}$$

$$HBut \leftrightarrow But^- + H^+ \quad k_{a5} = \frac{[But^-][H^+]}{[HBut]} \tag{A.29}$$

$$NH_4^+ \leftrightarrow NH_3 + H^+ \quad k_{a6} = \frac{[NH_3][H^+]}{[NH_4^+]} \tag{A.30}$$

$$H_2O \leftrightarrow OH^- + H^+ \quad k_w = [OH^-][H^+] \tag{A.31}$$

Ionic balance equations for both α and β liquid phases

$$\begin{aligned}[H^+] + [NH_4^+] = {} & [OH^-] + [HCO_3^-] + 2[CO_3^{2-}] \\ & + [Ac^-] + [Pr^-] + [But^-] + [A^-C^+]\end{aligned} \tag{A.32}$$

where

$$[NH_4^+] = \frac{C_{am}/17}{1 + k_{a6}/[H^+]} \tag{A.33}$$

$$[OH^-] = k_w/[H^+] \tag{A.34}$$

$$[HCO_3^-] = \frac{C_c/44}{1 + [H^+]/k_{a1} + k_{a2}/[H^+]} \tag{A.35}$$

$$[CO_2^{2-}] = \frac{C_c/44}{1 + [H^+]/k_{a2} + [H^+]^2/k_{a1}k_{a2}} \tag{A.36}$$

$$[Ac^-] = \frac{C_{ac}/60}{1 + [H^+]/k_{a3}} \tag{A.37}$$

$$[Pr^-] = \frac{C_{pr}/74}{1 + [H^+]/k_{a4}} \tag{A.38}$$

$$[But^-] = \frac{C_{but}/88}{1 + [H^+]/k_{a5}} \tag{A.39}$$

Appendix A. Material balances

A.1. Liquid phase

Microbial biomass, X_i, $i =$ A, AP, AB, M

$$\frac{\mathrm{d}X_i^\alpha}{\mathrm{d}t} = \frac{X_{i,\mathrm{f}} - X_i^\alpha}{a\theta} + \frac{X_i^\beta - X_i^\alpha}{a\theta/b} + (\mu_i^\alpha - b_i)X_i^\alpha \tag{A.1}$$

$$\frac{\mathrm{d}X_i^\beta}{\mathrm{d}t} = \frac{X_i^\alpha - X_i^\beta}{(1-a)\theta/b} + (\mu_i^\beta - b_i)X_i^\beta \tag{A.2}$$

Insoluble substrate, C_{is}

$$\frac{\mathrm{d}C_{\mathrm{is}}^\alpha}{\mathrm{d}t} = \frac{C_{\mathrm{is,f}} - C_{\mathrm{is}}^\alpha}{a\theta} + \frac{C_{\mathrm{is}}^\beta - C_{\mathrm{is}}^\alpha}{a\theta/b} - k^\alpha C_{\mathrm{is}}^\alpha \tag{A.3}$$

$$\frac{\mathrm{d}C_{\mathrm{is}}^\beta}{\mathrm{d}t} = \frac{C_{\mathrm{is}}^\alpha - C_{\mathrm{is}}^{\beta\alpha}}{(1-a)\theta/b} - k^\beta C_{\mathrm{is}}^\beta \tag{A.4}$$

Soluble substrate, C_{s}

$$\frac{\mathrm{d}C_{\mathrm{s}}^\alpha}{\mathrm{d}t} = \frac{C_{\mathrm{s,f}} - C_{\mathrm{s}}^\alpha}{a\theta} + \frac{C_{\mathrm{s}}^\beta - C_{\mathrm{s}}^\alpha}{a\theta/b} + \frac{162y_{\mathrm{e}}}{162+17n}k^\alpha C_{\mathrm{is}}^\alpha - 12.858\mu_{\mathrm{A}}^\alpha X_{\mathrm{A}}^\alpha \tag{A.5}$$

$$\frac{\mathrm{d}C_{\mathrm{s}}^\beta}{\mathrm{d}t} = \frac{C_{\mathrm{s}}^\alpha - C_{\mathrm{s}}^\beta}{(1-a)\theta/b} + \frac{162y_{\mathrm{e}}}{162+17n}k^\beta C_{\mathrm{is}}^\beta - 12.858\mu_{\mathrm{A}}^\beta X_{\mathrm{A}}^\beta \tag{A.6}$$

Total acetate, C_{ac}

$$\frac{\mathrm{d}C_{\mathrm{ac}}^\alpha}{\mathrm{d}t} = \frac{C_{\mathrm{ac,f}} - C_{\mathrm{ac}}^\alpha}{a\theta} + \frac{C_{\mathrm{ac}}^\beta - C_{\mathrm{ac}}^\alpha}{a\theta/b} + 3.54\mu_{\mathrm{A}}^\alpha X_{\mathrm{A}}^\alpha + 8.006\mu_{\mathrm{AP}}^\alpha X_{\mathrm{AP}}^\alpha + 15.366\mu_{\mathrm{AB}}^\alpha X_{\mathrm{AB}}^\alpha - 24.135\mu_{\mathrm{M}}^\alpha X_{\mathrm{M}}^\alpha \tag{A.7}$$

$$\frac{\mathrm{d}C_{\mathrm{ac}}^\beta}{\mathrm{d}t} = \frac{C_{\mathrm{ac}}^\alpha - C_{\mathrm{ac}}^\beta}{(1-a)\theta/b} + 3.54\mu_{\mathrm{A}}^\beta X_{\mathrm{A}}^\beta + 8.006\mu_{\mathrm{AP}}^\beta X_{\mathrm{AP}}^\beta + 15.366\mu_{\mathrm{AB}}^\beta X_{\mathrm{AB}}^\beta - 24.135\mu_{\mathrm{M}}^\beta X_{\mathrm{M}}^\beta \tag{A.8}$$

Total propionate, C_{pr}

$$\frac{\mathrm{d}C_{\mathrm{pr}}^\alpha}{\mathrm{d}t} = \frac{C_{\mathrm{pr,f}} - C_{\mathrm{pr}}^\alpha}{a\theta} + \frac{C_{\mathrm{pr}}^\beta - C_{\mathrm{pr}}^\alpha}{a\theta/b} + 2.937\mu_{\mathrm{A}}^\alpha X_{\mathrm{A}}^\alpha - 10.566\mu_{\mathrm{AP}}^\alpha X_{\mathrm{AP}}^\beta \tag{A.9}$$

$$\frac{\mathrm{d}C_{\mathrm{pr}}^\beta}{\mathrm{d}t} = \frac{C_{\mathrm{pr}}^\alpha - C_{\mathrm{pr}}^\beta}{(1-a)\theta/b} + 2.937\mu_{\mathrm{A}}^\beta X_{\mathrm{A}}^\beta - 10.566\mu_{\mathrm{AP}}^\beta X_{\mathrm{AP}}^\beta \tag{A.10}$$

Total butyrate, C_{but}

$$\frac{\mathrm{d}C_{\mathrm{but}}^\alpha}{\mathrm{d}t} = \frac{C_{\mathrm{but,f}} - C_{\mathrm{but}}^\alpha}{a\theta} + \frac{C_{\mathrm{but}}^\beta - C_{\mathrm{but}}^\alpha}{a\theta/b} + 3.079\mu_{\mathrm{A}}^\alpha X_{\mathrm{A}}^\alpha - 11.919\mu_{\mathrm{BP}}^\alpha X_{\mathrm{AB}}^\alpha \tag{A.11}$$

$$\frac{\mathrm{d}C_{\mathrm{but}}^\beta}{\mathrm{d}t} = \frac{C_{\mathrm{but}}^\alpha - C_{\mathrm{but}}^\beta}{(1-a)\theta/b} + 3.079\mu_{\mathrm{A}}^\beta X_{\mathrm{A}}^\beta - 11.919\mu_{\mathrm{BP}}^\beta X_{\mathrm{AB}}^\beta \tag{A.12}$$

Total ammonium, C_{am}

$$\frac{\mathrm{d}C_{\mathrm{am}}^{\alpha}}{\mathrm{d}t} = \frac{C_{\mathrm{am,f}} - C_{\mathrm{am}}^{\alpha}}{a\theta} + \frac{C_{\mathrm{am}}^{\beta} - C_{\mathrm{am}}^{\alpha}}{a\beta}\,\frac{17(n - m(1 - y_{\mathrm{e}}))}{162 + 17n} k^{\alpha} C_{\mathrm{is}}^{\alpha} - 0.15(\mu_{\mathrm{A}}^{\alpha} X_{\mathrm{A}}^{\alpha} + \mu_{\mathrm{AP}}^{\alpha} X_{\mathrm{AP}}^{\alpha} + \mu_{\mathrm{AB}}^{\alpha} X_{\mathrm{AB}}^{\alpha} + \mu_{\mathrm{M}}^{\alpha} X_{\mathrm{M}}^{\alpha}) \tag{A.13}$$

$$\frac{\mathrm{d}C_{\mathrm{am}}^{\beta}}{\mathrm{d}t} = \frac{C_{\mathrm{am}}^{\alpha} - C_{\mathrm{am}}^{\beta}}{(1-a)\theta/b} + \frac{17(n - m(1 - y_{\mathrm{e}}))}{162 + 17n} k^{\beta} C_{\mathrm{is}}^{\beta} - 0.15(\mu_{\mathrm{A}}^{\beta} X_{\mathrm{A}}^{\beta} + \mu_{\mathrm{AP}}^{\beta} X_{\mathrm{AP}}^{\beta} + \mu_{\mathrm{AB}}^{\beta} X_{\mathrm{AB}}^{\beta} + \mu_{\mathrm{M}}^{\beta} X_{\mathrm{M}}^{\beta}) \tag{A.14}$$

Total carbon dioxide in the liquid phase, C_{c}

$$\frac{\mathrm{d}C_{\mathrm{c}}^{\alpha}}{\mathrm{d}t} = \frac{C_{\mathrm{c,f}} - C_{\mathrm{c}}^{\alpha}}{a\theta} - \frac{C_{\mathrm{c}}^{\beta} - C_{\mathrm{c}}^{\alpha}}{a\theta/b} + 2.413\mu_{\mathrm{A}}^{\alpha} X_{\mathrm{A}}^{\alpha} + 1.01\mu_{\mathrm{AP}}^{\alpha} X_{\mathrm{AP}}^{\alpha} - 3.303\mu_{\mathrm{AB}}^{\alpha} X_{\mathrm{AB}}^{\alpha} + 16.726\mu_{\mathrm{M}}^{\alpha} X_{\mathrm{M}}^{\alpha} - \frac{N_{\mathrm{c}}^{\alpha}}{aV_{\mathrm{l}}} \tag{A.15}$$

$$\frac{\mathrm{d}C_{\mathrm{c}}^{\beta}}{\mathrm{d}t} = +\frac{C_{\mathrm{c}}^{\alpha} - C_{\mathrm{c}}^{\beta}}{(1-a)\theta/b} + 2.413\mu_{\mathrm{A}}^{\beta} X_{\mathrm{A}}^{\beta} + 1.01\mu_{\mathrm{AP}}^{\beta} X_{\mathrm{AP}}^{\beta} - 3.303\mu_{\mathrm{AB}}^{\beta} X_{\mathrm{AB}}^{\beta} + 16.726\mu_{\mathrm{M}}^{\beta} X_{\mathrm{M}}^{\beta} \tag{A.16}$$

Methane in the liquid phase, C_{m}

$$\frac{C_{\mathrm{m}}^{\beta}}{a\theta/b} + 1.509\mu_{\mathrm{AP}}^{\alpha} X_{\mathrm{AP}}^{\alpha} + 0.956\mu_{\mathrm{AB}}^{\alpha} X_{\mathrm{AB}}^{\alpha} + 6.082\mu_{\mathrm{M}}^{\alpha} X_{\mathrm{M}}^{\alpha} - \frac{N_{\mathrm{m}}^{\alpha}}{aV_{\mathrm{l}}} = 0 \tag{A.17}$$

$$\frac{\mathrm{d}C_{\mathrm{m}}^{\beta}}{\mathrm{d}t} = \frac{C_{\mathrm{m}}^{\beta}}{(1-a)\theta/b} + 1.509\mu_{\mathrm{AP}}^{\beta} X_{\mathrm{AP}}^{\beta} + 0.956\mu_{\mathrm{AB}}^{\beta} X_{\mathrm{AB}}^{\beta} + 6.082\mu_{\mathrm{M}}^{\beta} X_{\mathrm{M}}^{\beta} \tag{A.18}$$

where

$$\theta = \frac{V_{\mathrm{l}}}{Q_{\mathrm{f}}} \tag{A.19}$$

$$b = \frac{Q_{\mathrm{e}}}{Q_{\mathrm{f}}} \tag{A.20}$$

A.2. Gas phase

Carbon dioxide in the gas phase, P_{c}

$$\frac{\mathrm{d}P_{\mathrm{c}}}{\mathrm{d}t} = \frac{RT}{V_{\mathrm{g}}}\left(\frac{N_{\mathrm{c}}^{\alpha}}{44} - \frac{P_{\mathrm{c}}}{P}F_{\mathrm{t}}\right) \tag{A.21}$$

Methane in the gas phase, P_{m}

$$\frac{\mathrm{d}P_{\mathrm{m}}}{\mathrm{d}t} = \frac{RT}{V_{\mathrm{g}}}\left(\frac{N_{\mathrm{m}}^{\alpha}}{16} - \frac{P_{\mathrm{m}}}{P}F_{\mathrm{t}}\right) \tag{A.22}$$

Total material balance in the gas phase, F_{t}

$$F_{\mathrm{t}} = \frac{P}{P - P_{\mathrm{w}}}\left(\frac{N_{\mathrm{m}}^{\alpha}}{16} + \frac{N_{\mathrm{c}}^{\alpha}}{44}\right) \tag{A.23}$$

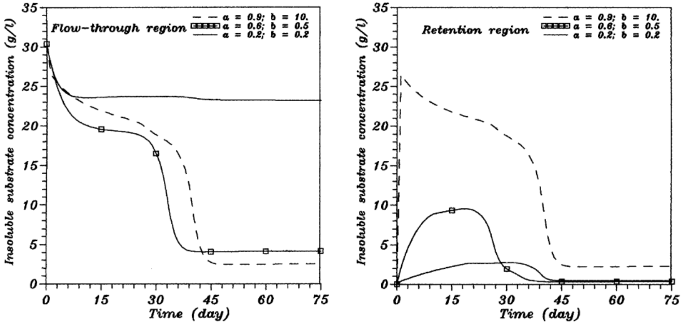

Fig. 2. Dynamic simulation of anaerobic digestion of cattle manure in a continuous flow reactor under HRT = 15 days and different degrees of mixing for prediction of the insoluble substrate concentration in flow-through and retention regions.

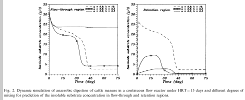

Models for cattle
Models for other herds
Models for management
Conclusion

ELSEVIER

Available online at www.sciencedirect.com
ScienceDirect

Livestock Science 106 (2007) 107 – 119

LIVESTOCK SCIENCE

www.elsevier.com/locate/livsci

Review article

Review of mathematical models for sow herd management

L.M. Plà *

R+D Centre, UdL-IRTA, Area of Animal Production, Rovira Roure, 198 E-25196 LLeida, Spain
University of Lleida, Department of Mathematics Jaume II, 73 E-25001 LLeida, Spain

Received 31 December 2005; received in revised form 26 August 2006; accepted 5 September 2006

Review article
Review of mathematical models for sow herd management
L.M. Plà *

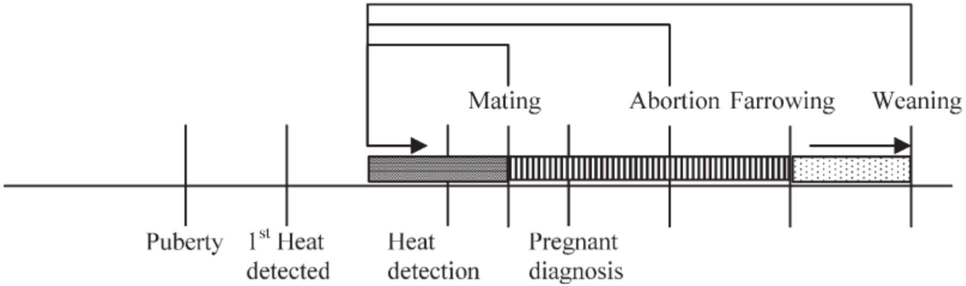

Fig. 1. Principal events and cyclic pattern in sow reproduction.

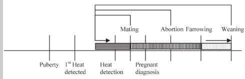

Fig. 1. Principal events and cyclic pattern in sow reproduction.

Main characteristics of sow herd models reviewed

Authors	Year	Aspects	Model	Title
Allen and Stewart	1983	R	S	A simulation model for a swine breeding unit producing feeder pigs
Tess et al.	1983	R, F, E	S	Simulation of genetic changes in life cycle efficiency of pork production I. A bioeconomic model
Dijkhuizen et al.	1986	RP, E	OP	Economic optimisation of culling strategies in swine breeding herds, using the "PORKCHOP computer program"
Marsh	1986	R, E	S	Economic decision making on health and management in livestock herds: examining complex problems through computer simulation
Pettigrew et al.	1986	R, E	S	Integration of factors affecting sow efficiency: a modelling approach
Signh	1986	R, E	S	Simulation of swine herd population dynamics
de Roo	1987	R, G, F	S	A stochastic model to study breeding schemes in a small pig population
Pomar et al.	1991	R, F	S	Computer simulation model of swine production systems: III. A dynamic herd simulation model including reproduction
Jalving et al.	1992	R, RP, E	S	Dynamic probabilistic modelling of reproduction and replacement management in sow herds. General aspects and model description
Huirne et al.	1993	R, RP, E	OP	An application of stochastic dynamic programming to support sow replacement decisions
Plà et al.	1998	R, RP, E	OP–S	A sow model for decision aid at farm level
Plà et al.	2003	R, E	S	A Markov decision sow model representing the productive lifespan of herd sows
Kristensen and Søllestad	2004a	R, RP, E	OP	A sow replacement model using Bayesian updating in a three-level hierarchic Markov process I. Biological model
	2004b			A sow replacement model using Bayesian updating in a three-level hierarchic Markov process II. Optimisation model

R: reproduction, RP: replacement, E: economics, F: feeding, G: genetics, S: simulation, O: optimisation.

Acta Scientiarum

http://www.uem.br/acta
ISSN printed: 1806-2636
ISSN on-line: 1807-8672
Doi: 10.4025/actascianimsci.v39i1.31366

Comparing non-linear mathematical models to describe growth of different animals

Jhony Tiago Teleken[1*], Alessandro Cazonatto Galvão[2] and Weber da Silva Robazza[2]

*[1]Departamento de Engenharia Química e de Alimentos, Universidade Federal de Santa Catarina, 88040-900, Florianópolis, Santa Catarina, Brazil. [2]Departamento de Engenharia de Alimentos e Engenharia Química, Universidade do Estado de Santa Catarina, Pinhalzinho, Santa Catarina, Brazil. *Author for correspondence. E-mail: jhony_tt@yahoo.com.br*

Acta Scientiarum
http://www.uem.br/acta
ISSN printed: 1806-2636
ISSN on-line: 1807-8672
Doi: 10.4025/actascianimsci.v39i1.31366

Comparing non-linear mathematical models to describe growth of different animals

Jhony Tiago Teleken[1*], Alessandro Cazonatto Galvão[2] and Weber da Silva Robazza[2]

[1]Departamento de Engenharia Química e de Alimentos, Universidade Federal de Santa Catarina, 88040-900, Florianópolis, Santa Catarina, Brazil. [2]Departamento de Engenharia de Alimentos e Engenharia Química, Universidade do Estado de Santa Catarina, Pinhalzinho, Santa Catarina, Brazil. *Author for correspondence. E-mail: jhony_tt@yahoo.com.br

Model	Equation	
Brody	$W(t) = W_\infty \left[1 + \left[\left(\frac{W_0}{W_\infty} \right) - 1 \right] \exp(-kt) \right]$	(1)
von Bertalanffy	$W(t) = W_\infty \left[1 + \left[\left(\frac{W_0}{W_\infty} \right)^{1/3} - 1 \right] \exp(-kt) \right]^3$	(2)
Logistic	$W(t) = \dfrac{W_\infty}{1 + \left[\left(\frac{W_\infty}{W_0} \right) - 1 \right] \exp(-kt)}$	(3)
Gompertz	$W(t) = W_\infty \exp\left[\ln\left(\frac{W_0}{W_\infty} \right) \exp(-kt) \right]$	(4)
Richards	$W(t) = \dfrac{W_\infty \cdot W_0}{\left[W_0^m + \left(W_\infty^m - W_0^m \right) \exp(-kt) \right]^{\frac{1}{m}}}$ for $m \neq 0$	(5)

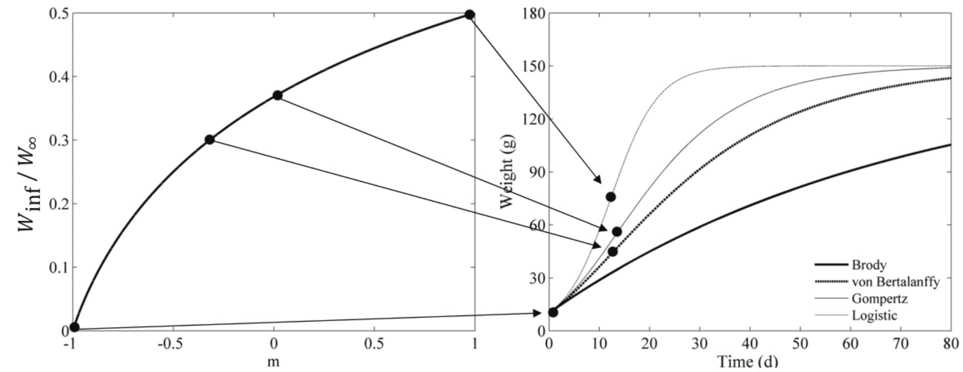

Figure 1. The influence of the parameter *m* on the inflection point of each growth curve: Brody (*m* = -1), von Bertalanffy (*m* = -1/3), Gompertz (*m* = 0), and Logistic (*m* = 1). The dots indicate the inflection points obtained for each growth model.

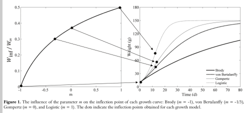

Table 1. Data sets used in this study to evaluate five different growth models.

Data set	Source
Holstein-Friesian bull[a]	Calo, Mcdowell, Vanvleck, and Miller, 1973 Table 1. Means and standard deviations for body weight, growth rates and degree of maturity of Holstein-Friesian bulls from 6 months to 8 years of age.
Nelore cow[b]	Silva, Alencar, Freitas, Packer, and Mourão, 2011 Figure 1. A) Estimation of weights based on age of Nelore females, observed and estimated by the models of Brody and von Bertalanffy.
Angus cow[b]	Beltrán, Butts, Olson, and Koger, 1992 Figure 1. Growth curves of Lines A and K estimated with Brody model. Line least squares means for weight at fixed ages are used as reference for goodness of fit.
Celta pig[b] (male and female)	Franco et al., 2011 Figure 2. Growth curve for males and females of the variety Barcina slaughtered at 14 months.
Karagouniko sheep[b] (male and female)	Goliomytis, Orfanos, Panopoulou, and Rogdakis, 2006 Figure 1. Growth curve and absolute growth rate for body weight of the Karagouniko male sheep: estimate growth curve; observed mean; estimated absolute growth rate. Figure 2. Growth curve and absolute growth rate for body weight of the Karagouniko female sheep: estimate growth curve; observed mean; estimated absolute growth rate.
Beetal goat[a] (male and female)	Waheed, Khan, Ali, and Sarwar, 2011 Table 1. Means (kg) and standard deviations (SD) of growth traits of Beetal goats.
New Zealand rabbit[a] Californian rabbit[a] Norfolk rabbit[a]	Curi, Nunes, and Curi, 1985 Table 2. Body weight of Norkfolk rabbit. Table 3. Body weight of Californian rabbit. Table 4. Body weight of New Zealand rabbit.
Athens-Canadian chicken[a] (male and female)	Aggrey, 2002 Table 1. Means and standard deviations for body weight at different ages in Athens-Canadian random-bred chickens.
Guinea fowl[a] (male and female)	Nahashon, Aggrey, Adefope, Amenyenu, and Wright, 2006 Table 2. Means and standard for body weight at different ages in a random-bred pearl guinea fowl population.
Japanese quail – white line[a] (male and female) Japanese quail – brown line[a] (male and female) Japanese quail – wild line[a] (male and female)	Sezer and Tarhan, 2005 Table 1. The results of statistical analyses for body weight of Japanese quail lines at different age (means ± standard errors).

[a]Experimental data reported in the literature; [b]Experimental data taken from published figures by means of GetData Graph Digitizer 2.24.

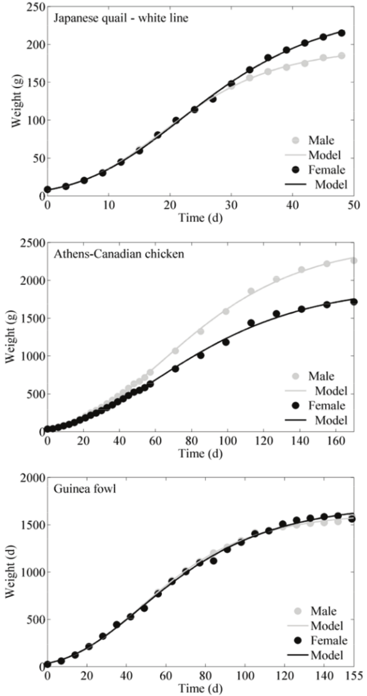

Figure 2. Birds growth kinetics fitted to the Richards' model.

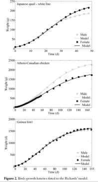

Table 6. Goodness of fit statistics obtained from the growth models applied to the experimental data set of mammals. Equations with the best goodness of fit are represented in bold.

Animals	Growth models				
	Eq.(1)	Eq.(2)	Eq.(3)	Eq.(4)	Eq.(5)
			Norfolk rabbit		
R^2	0.9925	**0.9991**	0.9950	0.9990	0.9992
RMSE	106.8	**37.30**	87.57	39.84	36.83
BIC	75.373	**58.922**	72.266	59.953	59.444
AIC_c	79.322	**62.870**	76.214	63.901	65.500
			Californian rabbit		
R^2	0.9882	0.9972	0.9943	**0.9976**	0.9976
RMSE	110.6	53.98	77.26	**49.91**	51.45
BIC	75.917	64.701	70.307	**63.477**	64.667
AIC_c	79.866	68.650	74.255	**67.425**	70.723
			New Zeland rabbit		
R^2	0.9909	**0.9985**	0.9942	0.9984	0.9986
RMSE	103.3	**42.07**	82.27	43.15	41.88
BIC	74.851	**60.803**	71.289	61.201	61.450
AIC_C	78.799	**64.752**	75.238	65.150	67.506
			Holstein-Friesian Bull		
R^2	0.9958	**0.9988**	0.9953	0.9986	0.9988
RMSE	17.54	**9.57**	18.61	10.02	9.60
BIC	67.549	**53.886**	68.892	54.910	54.872
AIC_C	70.395	**55.641**	71.738	57.756	59.117
			Nelore cow		
R^2	**0.9912**	0.9832	0.9641	0.9781	0.9922
RMSE	**14.84**	20.55	30.01	23.41	14.81
BIC	**29.856**	33.243	37.193	34.603	30.294
AIC_C	**35.6187**	39.006	42.955	40.365	39.691
			Angus cow		
R^2	**0.9981**	0.9921	0.9766	0.9878	0.9982
RMSE	**8.992**	18.26	31.47	22.68	9.955
BIC	**14.188**	18.497	21.804	19.813	14.778
AIC_C	**25.653**	29.961	33.268	31.277	39.397

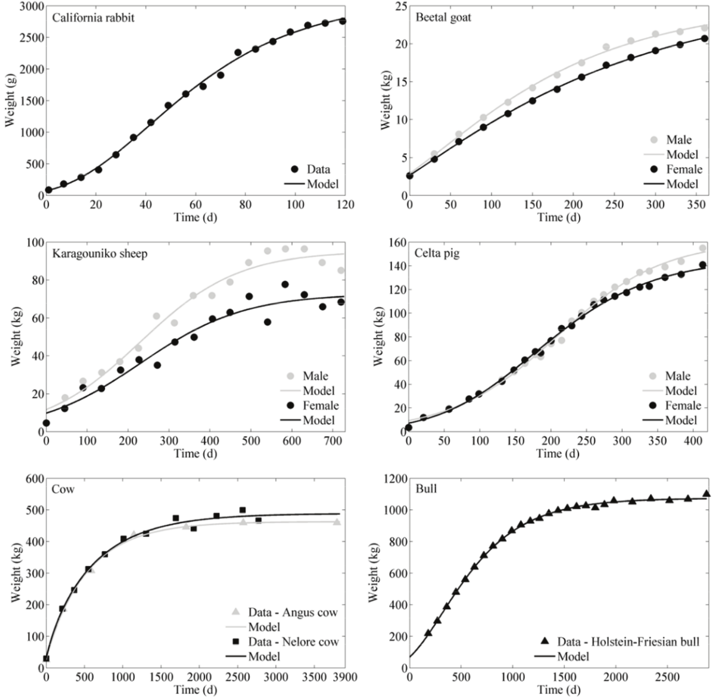

Figure 3. Mammals growth kinetics fitted to the Richards' model.

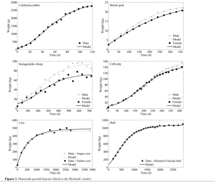

JOURNAL OF APPLIED ANIMAL RESEARCH
2021, VOL. 49, NO. 1, 158–166
https://doi.org/10.1080/09712119.2021.1915792

Taylor & Francis
Taylor & Francis Group

OPEN ACCESS Check for updates

Comparison of five mathematical models that describe growth in tropically adapted dual-purpose breeds of chicken

Oludayo Michael Akinsola [a], Emmanuel Babafunso Sonaiya [b], Oladeji Bamidele [b], Waheed Akinola Hassan [c], Abdulmojeed Yakubu [d], Folasade Olubukola Ajayi [e], Uduak Ogundu [f], Olayinka Olubunmi Alabi [g] and Oluwafunmilayo Ayoka Adebambo [h]

[a]Department of Theriogenology and Production, University of Jos, Jos, Nigeria; [b]African Chicken Genetic Gains Project National Secretariat, Department of Animal Science, Obafemi Awolowo University, Ile-Ife, Nigeria; [c]Department of Animal Science, Usmanu Danfodiyo University, Sokoto, Nigeria; [d]Department of Animal Science, Faculty of Agriculture, Nasarawa State University, Shabu-Lafia Campus Lafia, Keffi, Nigeria; [e]Department of Animal Science, University of Port-Harcourt, Port-Harcourt, Nigeria; [f]Department of Animal Science, Federal University of Technology, Owerri, Nigeria; [g]Department of Animal Science, Landmark University, Omu-Aran, Nigeria; [h]Department of Animal Breeding and Genetics, Federal University of Agriculture, Abeokuta, Nigeria

2023-04-17

Modelling livestock
└─Models for other herds

Table 1. Equations of the non-linear regression growth curve models.

Model	Equations	Age at inflection point	Weight at inflection point
Gompertz 3P	$Y = a.\exp(-\exp(-b.(age-c)))$	$\ln\frac{b}{a}$	$\frac{c}{e}$
Logistic 3P	$Y = \frac{c}{(1+\exp(-a\cdot(age-b)))}$	$-\ln\left(\frac{1}{b}\right)^{-a}$	$\frac{c}{2}$
Gompertz 4P	$Y = a + (b-a)\cdot\exp(-\exp(-c\cdot(age-d)))$	$\ln\left(\frac{d}{a}\right)$	$\frac{a}{e}.c$
Logistic 4P	$Y = c + \frac{d-c}{(1+\exp(-a\cdot(age-b)))}$	$\frac{c+d}{2}$	$\frac{d}{2}$

Notes: Y is the estimated weight at age x; a is the maturity index; b is the scale parameter; c is the asymptotic weight; d is the upper asymptote; Gompertz 3P was referenced from Gompertz (1832); Logistic 3P from Darmani et al. (2010); Logistic 4P from Ratwosky and Reddy (1986); Gompertz 4P from Tjørve and Tjørve (2017).

Materials and methods

Experimental site

The on-station test was conducted at Fol-Hope Farms, Ibadan, Oyo State and the Federal University of Agriculture, Abeokuta (FUNAAB), located within the Southern Guinea Savanna, and Dry Lowland Rainforest agro-ecological zones, respectively. The testing of the birds commenced in May 2016. The on-farm test was carried out in five agro-ecological zones as follows: Kebbi State (Sudan and Northern Guinea Savanna), Kwara State (Southern Guinea Savanna), Nasarawa State (Southern Guinea Savanna), Imo State (Wet Lowland Rain Forest and Fresh Water Swamp) and Rivers State (Mangrove Swamp and Fresh Water Swamp).

Management systems

A total of 1939 d-old chicks of both locally sourced breeds (Fulani, FUNAAB Alpha, Noiler and Shika-Brown) and imported breeds (Kuroiler and Sasso) were brooded to 42 days (Table 2). The birds were sexed at 42 days, and males and females were grown separately until 140 days under station (intensive production system) conditions. The stocking density was 10 chicks/m^2, seven birds/m^2, and five birds/m^2 during 0–42d, 43–91d and 92–140d, respectively. Commercial feed (Chick mash at 0–42d: 2,993 kcal ME/kg, 22.3% CP and Grower mash at 43–140d: 3013 kcal ME/kg, 17% CP) and water were available *ad libitum*. Birds in both stations were fed the same proprietary feed. Standard biosecurity measures and vaccination schedules were observed at the test centres. Body weight was measured every two weeks. For the on-farm test, a total of 58,639 six-weeks-old pre-vaccinated chickens were distributed to 2100

Materials and methods
Experimental site
The on-station test was conducted at Fol-Hope Farms, Ibadan, Oyo State and the Federal University of Agriculture, Abeokuta (FUNAAB), located within the Southern Guinea Savanna, and Dry Lowland Rainforest agro-ecological zones, respectively. The testing of the birds commenced in May 2016. The on-farm test was carried out in five agro-ecological zones as follows: Kebbi State (Sudan and Northern Guinea Savanna), Kwara State (Southern Guinea Savanna), Nasarawa State (Southern Guinea Savanna), Imo State (Wet Lowland Rain Forest and Fresh Water Swamp) and Rivers State (Mangrove Swamp and Fresh Water Swamp).
Management systems
A total of 1939 d-old chicks of both locally sourced breeds (Fulani, FUNAAB Alpha, Noiler and Shika-Brown) and imported breeds (Kuroiler and Sasso) were brooded to 42 days (Table 2). The birds were sexed at 42 days, and males and females were grown separately until 140 days under station (intensive production system) conditions. The stocking density was 10 chicks/m^2, seven birds/m^2, and five birds/m^2 during 0–42d, 43–91d and 92–140d, respectively. Commercial feed (Chick mash at 0–42d: 2,993 kcal ME/kg, 22.3% CP and Grower mash at 43–140d: 3013 kcal ME/kg, 17% CP) and water were available ad libitum. Birds in both stations were fed the same proprietary feed. Standard biosecurity measures and vaccination schedules were observed at the test centres. Body weight was measured every two weeks. For the on-farm test, a total of 58,639 six-weeks-old pre-vaccinated chickens were distributed to 2100

households across five states representing different agro-ecologies (Table 3). Standard backyard scavenging management practices were followed by the farmers with the addition of overnight housing, feed supplementation and vaccination programmes. Body weight was taken every four weeks.

All applicable veterinary permits were obtained for the importation and use of the imported breeds for research purposes (Bamidele et al. 2019). Both the on-station and on-farm studies were approved by the International Livestock Research Institute (ILRI) Institutional Research Ethics Committee (IREC) with reference no.: ILRI-IREC2015-08/1, and ILRI Institutional Animal Care and Use Committee (IACUC) with reference number: ILRI-IACUC-RC2016.2. Each farmer gave written informed consent to participate in the study.

households across five states representing different agro-ecologies (Table 3). Standard backyard scavenging management practices were followed by the farmers with the addition of overnight housing, feed supplementation and vaccination programmes. Body weight was taken every four weeks.

All applicable veterinary permits were obtained for the importation and use of the imported breeds for research purposes (Bamidele et al. 2019). Both the on-station and on-farm studies were approved by the International Livestock Research Institute (ILRI) Institutional Research Ethics Committee (IREC) with reference no.: ILRI-IREC2015-08/1, and ILRI Institutional Animal Care and Use Committee (IACUC) with reference number: ILRI-IACUC-RC2016.2. Each farmer gave written informed consent to participate in the study.

Table 5. Estimated growth curve parameters of female birds raised on-station from 0 to 20 weeks.

Breed/model	a	b	c	d	Age and weight at inflection point	AIC	BIC	RMSE	*AdjR*^{2}
Fulani									
Logistic 4P	0.26	11.35	−38.10	1429.00	10; 452.42	90.350	80.340	6.779	0.995
Logistic 3P	0.28	11.38		1109.22	10; 446.99	95.497	90.422	11.183	0.992
Gompertz 3P	0.14	10.46		1347.86	10; 463.54	99.351	94.276	13.324	0.989
Gompertz 4P	0.16	10.41	24.80	1292.41	10; 461.67	102.561	92.550	11.809	0.988
Neural network					10; 469.75			5.933	0.992
FUNAAB Alpha									
Logistic 3P	0.40	10.41		2780.35	10;1030.22	121.831	116.756	37.019	0.994
Gompertz 3P	0.20	9.07		2735.53	10;1070.99	125.555	120.480	43.846	0.990
Logistic 4P	0.30	10.32	−49.12	2247.55	10;1037.22	126.763	116.753	35.482	0.990
Gompertz 4P	0.22	9.21	59.16	2392.08	10;1067.04	128.188	118.177	37.856	0.989
Neural network					10;1084.91			38.829	0.990
Sasso									
Gompertz 3P	0.14	10.89		3856.63	10;1240.85	127.704	122.629	48.346	0.997
Gompertz 4P	0.14	10.88	7.06	3838.13	10;1240.36	135.016	125.006	51.633	0.992
Logistic 3P	0.28	11.76		3155.02	10;1192.88	138.815	133.740	80.110	0.988
Logistic 4P	0.23	11.82	−232.47	3412.27	10;1221.52	139.646	129.635	63.726	0.987
Neural network					10;1261.09			38.913	0.997
Kuroiler									
Gompertz 3P	0.14	10.40		3725.38	10;1292.28	119.769	114.694	33.706	0.995
Gompertz 4P	0.14	10.43	−23.13	3777.74	10;1293.34	126.740	116.729	35.444	0.991
Logistic 4P	0.21	11.38	−300.25	3385.91	10;1276.43	132.982	122.972	47.074	0.990
Logistic 3P	0.28	11.41		3090.09	10;1246.74	137.304	132.228	74.792	0.985
Neural network					10;1290.89			17.773	0.996
Shika-Brown									
Gompertz 3P	0.17	10.09		2088.27	10; 756.01	115.702	110.627	28.016	0.998
Logistic 3P	0.32	11.27		1803.37	10; 722.05	116.621	111.546	29.213	0.998
Logistic 4P	0.29	11.19	−58.62	1847.41	10; 732.26	118.844	108.833	24.756	0.998
Gompertz 4P	0.18	10.13	32.93	2034.90	10; 752.68	120.354	110.343	26.514	0.995
Neural network					10; 712.52			7.287	0.998
Noiler									
Gompertz 3P	0.18	7.97		2917.67	13;1955.35	105.461	92.445	58.794	0.992
Logistic 3P	0.27	9.66	30.33	2742.17	13;1959.03	108.221	95.206	69.867	0.990
Logistic 4P	0.13	0.44	−5131.7	3139.89	13;1947.59	122.384	92.781	58.948	0.989
Gompertz 4P	0.12	0.22	−3231.4	3204.77	13;1946.85	122.442	92.839	59.162	0.989
Neural network					13;1916.49			49.327	0.990

Notes: AIC: akaike information criterion; BIC: Bayesian information criterion; RMSE: root mean square error; AdjR^2: adjusted coefficient of determination; *a*is the maturity index; *b*is the scale parameter; *c*is the asymptotic weight; *d* is the upper asymptote. Non-linear model adapted from JMP 13.2 statistical software.

Heterogeneous herds

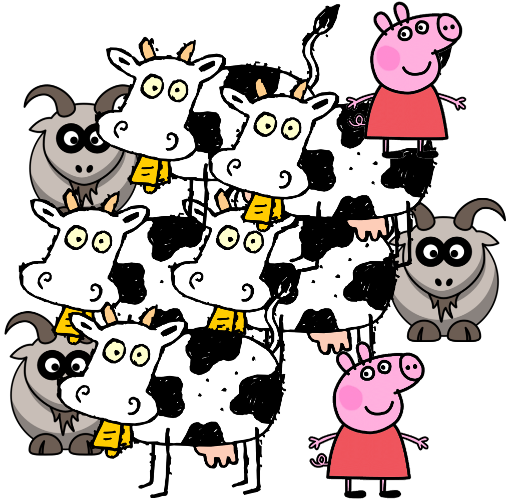

Heterogeneous herds

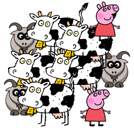

Livestock Science 157 (2013) 280–288

Contents lists available at ScienceDirect

Livestock Science

journal homepage: www.elsevier.com/locate/livsci

A mathematical model of the dynamics of Mongolian livestock populations

Duncan Shabb [a], Nakul Chitnis [a], Zolzaya Baljinnyam [a,b], Sansar Saagii [c], Jakob Zinsstag [a,*]

[a] Swiss Tropical and Public Health Institute/University of Basel, Socinstr. 57, P.O. Box 4002 Basel, Switzerland
[b] Institute of Veterinary Medicine, Mongolian State University of Agriculture, Ulaanbaatar, Mongolia
[c] Amin Nutag Orgil NGO, Ulaanbaatar, Mongolia

Livestock Science 157 (2013) 280–288
Contents lists available at ScienceDirect
Livestock Science
journal homepage: www.elsevier.com/locate/livsci
A mathematical model of the dynamics of Mongolian livestock populations
Duncan Shabb [a], Nakul Chitnis [a], Zolzaya Baljinnyam [a,b], Sansar Saagii [c], Jakob Zinsstag [a,*]

The state variables for total population at time t of goats sheep, cattle and horses are denoted G, S, C, and H respectively

$$G(t) = \sum_{i=1}^{3} X_{ig}(t) + Y_{ig}(t),$$

$$S(t) = \sum_{i=1}^{3} X_{is}(t) + Y_{is}(t),$$

$$C(t) = \sum_{i=1}^{3} X_{ic}(t) + Y_{ic}(t),$$

$$H(t) = \sum_{i=1}^{3} X_{ih}(t) + Y_{ih}(t), \tag{1}$$

with the juvenile population of cattle given by

$$X_{2c} = \sum_{\xi \in \{a,b\}} X_{2c\xi},$$

$$Y_{2c} = \sum_{\xi \in \{a,b\}} Y_{2c\xi},$$

The state variables for total population at time t of goats sheep, cattle and horses are denoted G, S, C, and H respectively

$$G(t) = \sum_{i=1}^{3} X_{ig}(t) + Y_{ig}(t),$$

$$S(t) = \sum_{i=1}^{3} X_{is}(t) + Y_{is}(t),$$

$$C(t) = \sum_{i=1}^{3} X_{ic}(t) + Y_{ic}(t),$$

$$H(t) = \sum_{i=1}^{3} X_{ih}(t) + Y_{ih}(t), \tag{1}$$

with the juvenile population of cattle given by

$$X_{2c} = \sum_{\xi \in \{a,b\}} X_{2c\xi},$$

$$Y_{2c} = \sum_{\xi \in \{a,b\}} Y_{2c\xi},$$

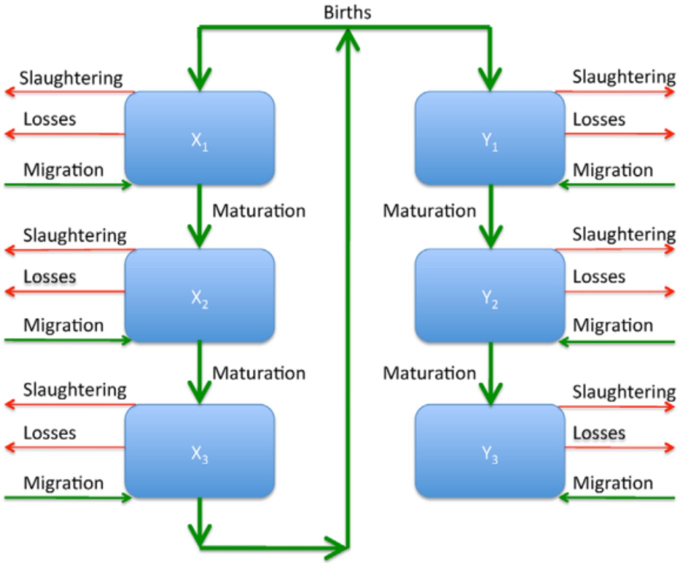

Fig. 1. Goat model dynamics. Arrows represent flows of animals into or out of the population. Boxes represent state variables. The figure is meant to be a simple conceptualization of the model dynamics. Sheep are modeled with an equivalent schematic but cattle and horses have additional juvenile stages.

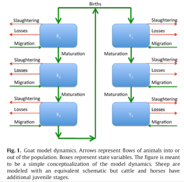

The model equations for goats are given by

$$X_{1g}(t+1) = b_g X_{3g}(t) + \frac{m_g X_{1g}(t)}{G(t)}, \tag{3a}$$

$$X_{2g}(t+1) = \frac{X_{1g}(t)}{(1+\alpha_g d_{X_{1g}} A(t)) k_{X_{1g}}} + \frac{m_g X_{2g}(t)}{G(t)}, \tag{3b}$$

$$X_{3g}(t+1) = \frac{X_{2g}(t)}{(1+\alpha_g d_{X_{2g}} A(t)) k_{X_{2g}}} + \frac{X_{3g}(t)}{(1+\alpha_g d_{X_{3g}} A(t)) k_{X_{3g}}} + \frac{m_g X_{3g}(t)}{G(t)}, \tag{3c}$$

$$Y_{1g}(t+1) = b_g X_{3g}(t) + \frac{m_g Y_{1g}(t)}{G(t)}, \tag{3d}$$

$$Y_{2g}(t+1) = \frac{Y_{1g}(t)}{(1+\alpha_g d_{Y_{1g}} A(t)) k_{Y_{1g}}} + \frac{m_g Y_{2g}(t)}{G(t)}, \tag{3e}$$

$$Y_{3g}(t+1) = \frac{Y_{2g}(t)}{(1+\alpha_g d_{Y_{2g}} A(t)) k_{Y_{2g}}} + \frac{Y_{3g}(t)}{(1+\alpha_g d_{Y_{3g}} A(t)) k_{Y_{3g}}} + \frac{m_g Y_{3g}(t)}{G(t)}. \tag{3f}$$

The model equations for goats are given by

$$X_{1g}(t+1) = b_g X_{3g}(t) + \frac{m_g X_{1g}(t)}{G(t)}, \tag{3a}$$

$$X_{2g}(t+1) = \frac{X_{1g}(t)}{(1+\alpha_g d_{X_{1g}} A(t)) k_{X_{1g}}} + \frac{m_g X_{2g}(t)}{G(t)}, \tag{3b}$$

$$X_{3g}(t+1) = \frac{X_{2g}(t)}{(1+\alpha_g d_{X_{2g}} A(t)) k_{X_{2g}}} + \frac{X_{3g}(t)}{(1+\alpha_g d_{X_{3g}} A(t)) k_{X_{3g}}} + \frac{m_g X_{3g}(t)}{G(t)}, \tag{3c}$$

$$Y_{1g}(t+1) = b_g X_{3g}(t) + \frac{m_g Y_{1g}(t)}{G(t)}, \tag{3d}$$

$$Y_{2g}(t+1) = \frac{Y_{1g}(t)}{(1+\alpha_g d_{Y_{1g}} A(t)) k_{Y_{1g}}} + \frac{m_g Y_{2g}(t)}{G(t)}, \tag{3e}$$

$$Y_{3g}(t+1) = \frac{Y_{2g}(t)}{(1+\alpha_g d_{Y_{2g}} A(t)) k_{Y_{2g}}} + \frac{Y_{3g}(t)}{(1+\alpha_g d_{Y_{3g}} A(t)) k_{Y_{3g}}} + \frac{m_g Y_{3g}(t)}{G(t)}. \tag{3f}$$

Table 1
Description of types parameters of the model for livestock population dynamics. The model consists of five basic parameters that are further subdivided by species out of which some are further subdivided by age and sex.

Parameter	Description	Level
b	Expected number of female offspring per one adult female over one year. Dimensionless	Species
m	Number of new animals entering the area in one year. Dimension: Animals	Species
α	Species-dependent resource availability. Dimension: 1/Animals	Species
d	Modulation of resource availability by age and sex of animal. Dimensionless	Species, sex, age
k	Reciprocal of per capita survival excluding the effects of density-dependent mortality. Dimensionless	Species, sex, age
c	Weighting of food consumption by animals. Dimensionless	Species, age

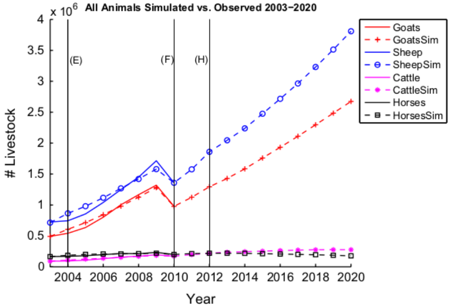

Fig. 2. All species population dynamics of observed and simulated data for periods (E)–(H).

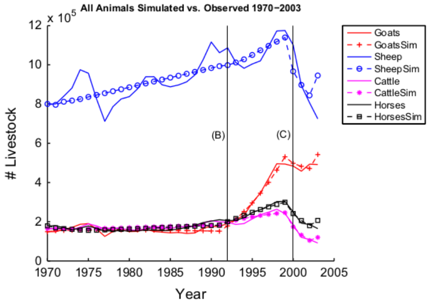

Fig. 3. All species population dynamics of observed and simulated data of periods (A)–(D).

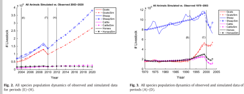

Models for cattle

Models for other herds

Models for management

Conclusion

2023-04-17

Modelling livestock
└─Models for management

Animal Science Journal (2010) **81,** 411–424 doi: 10.1111/j.1740-0929.2010.00769.x

REVIEW ARTICLE

Systems approaches to beef cattle production systems using modeling and simulation

Hiroyuki HIROOKA

Graduate School of Agriculture, Kyoto University, Sakyo, Kyoto, Japan

ABSTRACT

Systems approach techniques have been applied to modeling production systems for beef cattle from the relatively micro-level of tissues and organs to the macro-level of farms and geographical regions. This paper reviews the various types of beef cattle production models already in operation in order to analyze beef cattle production systems and their components. It may be theoretically possible to construct system models which describe such complex production systems and can be generally used in various genetic, nutritional, management and economic situations as well as in training, extension and educational programs. Moreover, the systems approach can assist in the organization of information and identification of knowledge gaps and thereby open an avenue to multi-disciplinary research projects.

Key words: *beef cattle, model, simulation, systems approach.*

Animal Science Journal (2010) 81, 411–424 doi: 10.1111/j.1740-0929.2010.00769.x
REVIEW ARTICLE
Systems approaches to beef cattle production systems using modeling and simulation
Hiroyuki HIROOKA
Graduate School of Agriculture, Kyoto University, Sakyo, Kyoto, Japan
ABSTRACT
Systems approach techniques have been applied to modeling production systems for beef cattle from the relatively micro-level of tissues and organs to the macro-level of farms and geographical regions. This paper reviews the various types of beef cattle production models already in operation in order to analyze beef cattle production systems and their components. It may be theoretically possible to construct system models which describe such complex production systems and can be generally used in various genetic, nutritional, management and economic situations as well as in training, extension and educational programs. Moreover, the systems approach can assist in the organization of information and identification of knowledge gaps and thereby open an avenue to multi-disciplinary research projects.
Key words: beef cattle, model, simulation, systems approach.

Ann. Anim. Sci., Vol. 10, No. 4 (2010) 333–348

APPLICATION OF MATHEMATICAL MODELLING IN BEEF HERD MANAGEMENT – A REVIEW*

Anna Stygar, Joanna Makulska

Department of Cattle Breeding, University of Agriculture in Kraków, Al. Mickiewicza 24/28, 30-059 Kraków, Poland
Corresponding author: rzmakuls@cyf-kr.edu.pl

Ann. Anim. Sci., Vol. 10, No. 4 (2010) 333–348

APPLICATION OF MATHEMATICAL MODELLING IN BEEF HERD MANAGEMENT – A REVIEW*

Anna Stygar, Joanna Makulska

Department of Cattle Breeding, University of Agriculture in Kraków, Al. Mickiewicza 24/28, 30-059 Kraków, Poland
Corresponding author: rzmakuls@cyf-kr.edu.pl

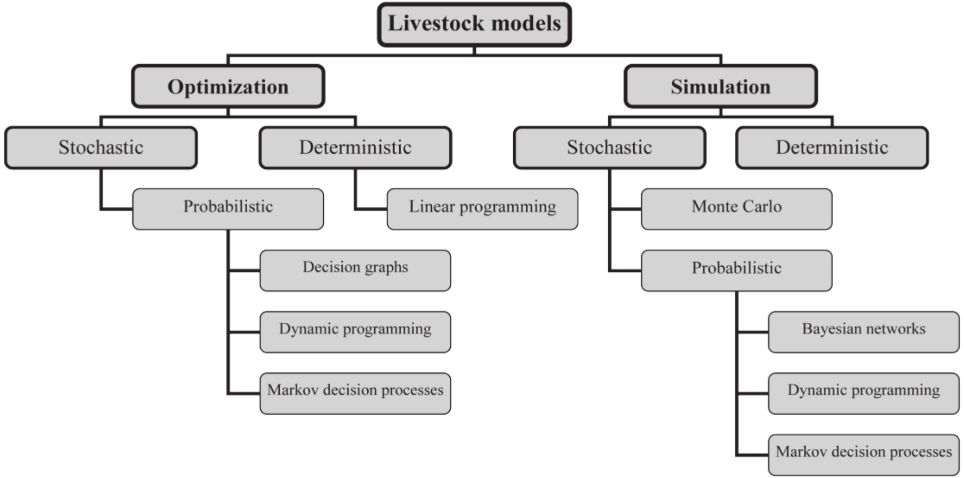

Figure 1. Methodological classification of livestock models

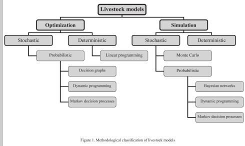

Journal of Animal Science, 2022, **100**, 1–19
https://doi.org/10.1093/jas/skac160
Advance access publication 3 May 2022
Board Invited Reviews

OXFORD

AMERICAN SOCIETY OF ANIMAL SCIENCE

ASAS–NANP Symposium: Mathematical Modeling in Animal Nutrition: Opportunities and challenges of confined and extensive precision livestock production

Hector M. Menendez III,[†,1] Jameson R. Brennan,[†] Charlotte Gaillard,[‡] Krista Ehlert,[||] Jaelyn Quintana,[†] Suresh Neethirajan,[$] Aline Remus,[¶] Marc Jacobs,[**] Izabelle A. M. A. Teixeira,[††] Benjamin L. Turner,[‡‡] and Luis O. Tedeschi[|||]

[†]Department of Animal Science, South Dakota State University, Rapid City, SD 57702, USA
[‡]Institut Agro, PEGASE, INRAE, 35590 Saint Gilles, France
[||]Department of Natural Resource Management, South Dakota State University, Rapid City, SD, 57702, USA
[$]Farmworx, Adaptation Physiology, Animal Sciences Group, Wageningen University, 6700 AH, The Netherlands
[¶]Sherbrooke Research and Development Centre, Sherbrooke, QC J1M 1Z3, Canada
[**]FR Analytics B.V., 7642 AP Wierden, The Netherlands
[††]Department of Animal, Veterinary, and Food Sciences, University of Idaho, Twin Falls, ID 83301, USA
[‡‡]Department of Agriculture, Agribusiness, and Environmental Science, King Ranch® Institute for Ranch Management, Texas A&M University-Kingsville, Kingsville, TX 78363, USA
[|||]Department of Animal Science, Texas A&M University, College Station, TX 77843-2471, USA
[1]Corresponding author: hector.menendez@sdstate.edu

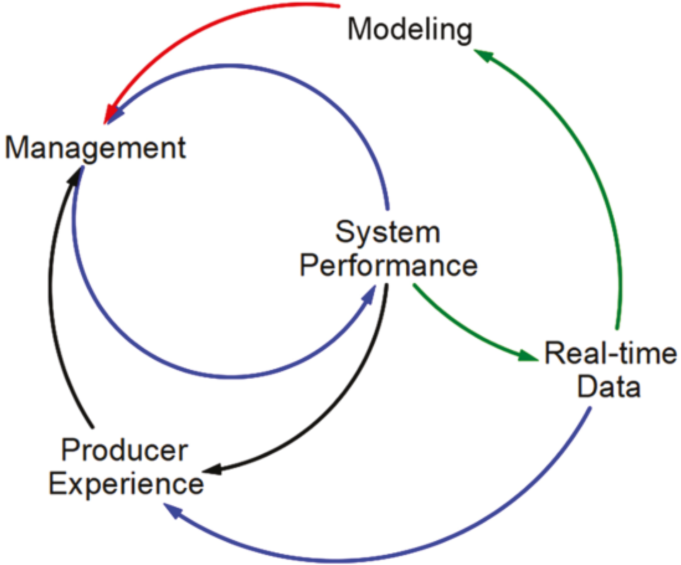

Figure 1. Diagram of the conventional producer decision process, including mental models (producer experience) and the role of modeling in relation to real-time data integration.

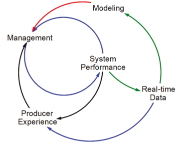

Figure 1. Diagram of the conventional producer decision process, including mental models (producer experience) and the role of modeling in relation to real-time data integration.

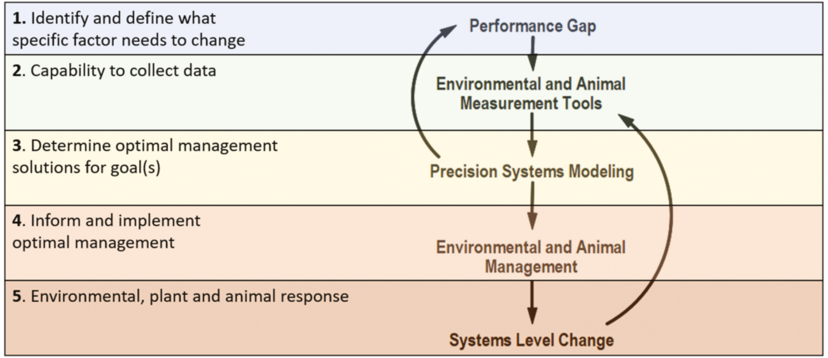

Figure 2. Conceptual diagram of five principles for sustainable precision livestock implementation using precision measurement and management tools integrated with mathematical models.

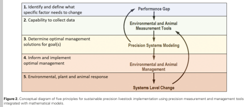

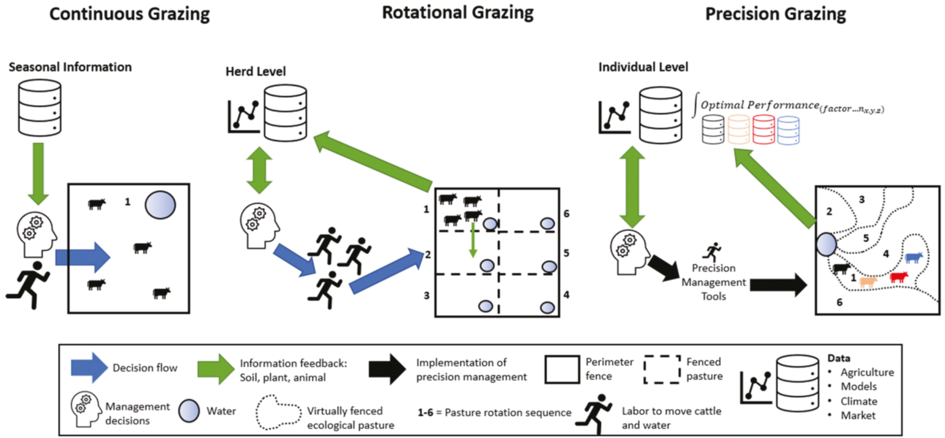

Figure 3. Continuous vs. rotational grazing as each relates to decision flow, information feedback, and management decisions, labor, and data.

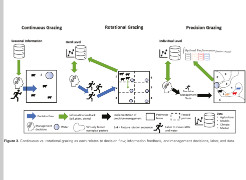

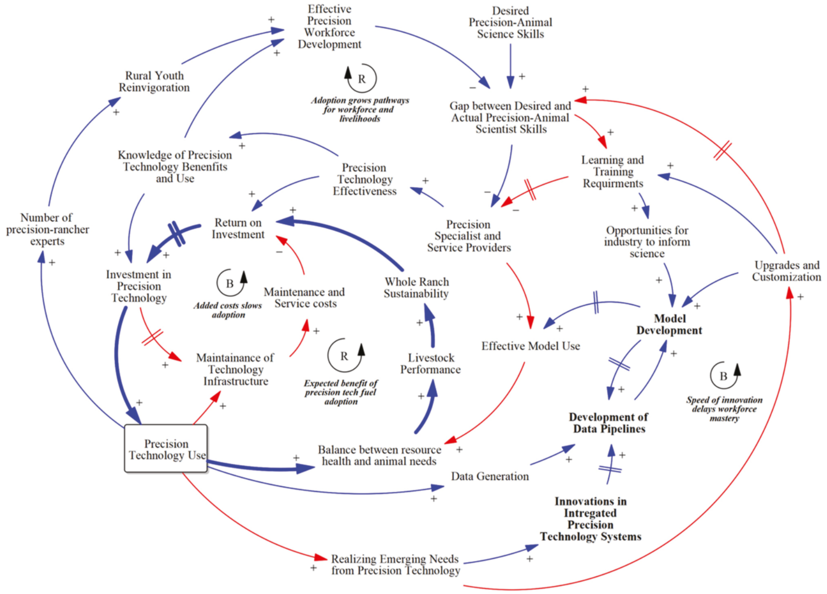

Figure 5. Causal loop diagram of precision livestock integration through precision system models, education workforce development, and producer and industry synergies. A positive (+) relationship between variables indicates that as the value of the arrowhead moves in the same direction (increases or decreases) as the variable at the tail (e.g., as Precision Technology Use increases, the Maintenance of Technology Infrastructure also increases). A negative (–) relationship between variables indicates that the variable at the arrowhead moves in the opposite direction of the variable at the tail (e.g., as Learning and Training Requirements increases, the number of Precision Specialist and Service Providers decreases). The double perpendicular lines on arrows represent time delays between variable responses. The R and B labels identify reinforcing (positive feedback) or balancing (negative feedback) relationships.

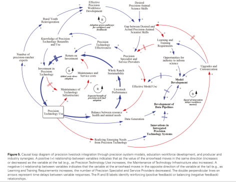

Table 1. Real-time models found in the literature using the search keywords: real-time, animal science, nutrition, and modeling

Author	Aim	Target	Type	Response
Hauschild et al. (2012, 2020); Remus et al. (2020c)	Provide daily tailored diets to individuals	Growing pigs	Gray box (empirical [data-driven] and mechanistic)	Diet composition to sustain observed growth
Peña Fernández et al. (2019)	Predict in real-time the indoor particle sizes concentration	Poultry	Data-based mechanistic	Predicted indoor particle sizes concentration
Parsons et al. (2007)	Integrated control of pig growth and pollutant emissions	Growing pigs	Data-based mechanistic	Predicted growth response based on diet intake
Stacey et al. (2004)	Control of broiler growth and nutrition	Broiler	Semi-mechanistic	Predicted growth response based on diet intake and control nutrient intake
Fu et al. (2020)	Predict diet energy digestion	Dairy cows	Kernel extreme learning machine	Predicted digestible energy and energy digestibility
Kashiha et al. (2013)	Report malfunctioning in a broiler house to the farmer in real time	Broiler	Empirical (data-driven)	Prediction of the distribution index of broilers
Gauthier et al. (2019); Gaillard et al. (2020b)	Provide daily tailored diets to individuals	Sows	Gray box (empirical [data-driven] and mechanistic)	Diet composition to sustain fetus development and milk production

Models for cattle
Models for other herds
Models for management
Conclusion

Conclusion

Many interesting models

(Many models have never been "properly" studied mathematically and are "waiting" for an analysis)

I showed only one statistical model, but the majority of published work used to be statistical

Contrary to other fields: easy to generate data of good quality

I voluntarily excluded disease-related works.. but they are easy to find!

Conclusion

Many interesting models

(Many models have never been "properly" studied mathematically and are "waiting" for an analysis)

I showed only one statistical model, but the majority of published work used to be statistical

Contrary to other fields: easy to generate data of good quality

I voluntarily excluded disease-related works.. but they are easy to find!